Circuit Simulator Based Mextram Parameter Extraction of SiGe HBTs

by

Yili Wang

A thesis submitted to the Graduate Faculty of
Auburn University
in partial fulfillment of the
requirements for the Degree of
Master of Science

Auburn, Alabama
May 7, 2016

Keywords: Mextram SiGe HBT, Parameter Extraction, ICCAP

Approved by

Guofu Niu, Professor of Electrical and Computer Engineering
Fa Foster Dai, Professor of Electrical and Computer Engineering
Michael C. Hamilton, Associate Professor of Electrical and Computer Engineering

Abstract

This work implements Mextram 504 parameter extraction using ICCAP and ADS simulator. A 50 GHz SiGe HBT is used. Results show a whole procedure of parameter extraction with temperature scaling.

Acknowledgments

I would like to express my deepest appreciation to my advisor Dr. Guofu Niu for his full support, expert guidance and encouragement throughout my study. Without his guidance and persistent help this dissertation would not have been possible. In addition, I express my gratitude to Dr. Dai and Dr. Hamilton for their thoughtful comments and precious time.

I am very much thankful to my group mates for their support and encouragement.

Finally, I would like to acknowledge with gratitude, the support and love of my family, and my God. They are the power that help me work through everything.

Table of Contents

List of Figures

List of Tables

Chapter 1

Introduction

1.1 SiGe HBT fundamentals

The Silicon-Germanium heterojunction bipolar transistor (SiGe HBT) has gained world-wide attention, since it could get higher current gain, higher cut-off frequency and lower base resistance compared with Si BJT. The heart of SiGe technology is a SiGe hetrojunction bipolar transistor (HBT), which is the first practical bandgap engineering device realized in silicon,is easy to integrated with modern CMOS technology. Adding Ge to Si BJT intro-

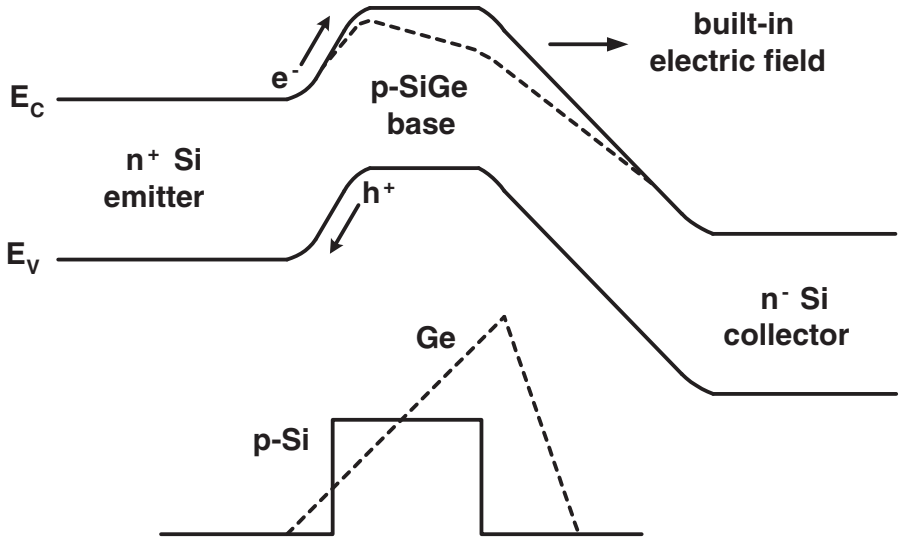

Figure 1.1: Energy band diagrams of a graded-base SiGe HBT and an Si BJT [1]

duced a number of exciting performance improvements. The base region of SiGe HBTs is typically the region where SiGe alloy is used instead of Si. The basic operational principle of SiGe HBT can be best understood by considering the band diagram shown in Figure 1.1. It illustrates the difference between SiGe HBT and Si BJT by showing the energy-band

diagrams for both SiGe HBT and Si BJT biased identically in forward-active mode. The Ge profile linearly increases from zero near emitter-base (EB) junction to some maximum value near collector-base (CB) junction, and then rapidly ramps down to zero [2]. Since the energy bandgap of Ge is smaller than that of Si, adding germanium into the base region of the transistor leads to an additional bandgap shrinkage, which is approximately 75 meV for each 10 percent of Ge introduced[3]. The reduction of bandgap decreases band transit time, which gives a higher f_T. Smaller base bandgap also increases electron injection, which leads to a higher β. At same collector current density, compared with normal BJT, SiGe HBT allows us to have a higher base region doping concentration, which reduces base resistance.

1.2 Mextram basics

Mextram model is a widely used vertical bipolar transistor model. It contains many features that the widely-used Ebers-Moll and Gummel-Poon model lacks. Mextram is the acronym of the "most exquisite transistor model". The first Mextram release was introduced as Level 501 in 1985. Later Level 502, 503 and 504 were respectively released in 1986 , 1994 and 2000. And development was never stopped following the requirement of updated technology. The latest accessible version is Level 504.12[4] . Mextram contains descriptions for the following effects:

- Bias-dependent Early effect
- Low-level non-ideal base currents
- High-injection effects
- Ohmic resistance of the epilayer
- Velocity saturation effects on the resistance of the epilayer
- Hard and quasi-saturation (including Kirk effect)
- Weak avalanche in the collector-base junction (optionally including snap-back behaviour)

- Zener-tunneling current in the emitter-base junction
- Charge storage effects
- Split base-collector and base-emitter depletion capacitance
- Substrate effects and parasitic PNP
- Explicit modelling of inactive regions
- Current crowding and conductivity modulation of the base resistance
- First order approximation of distributed high frequency effects in the intrinsic base (high-frequency current crowding and excess phase-shift)
- Recombination in the base (meant for SiGe transistors)
- Early effect in the case of a graded bandgap (meant for SiGe transistors)
- Temperature scaling
- Self-heating
- Thermal noise, shot noise and $1/f$-noise

In the latest Mextram model, there are five internal nodes and 93 parameters, including parameters of model flag, parameters of noise and the reference temperature, and parameters of temperature scaling.

Some parts of the model are optional and can be switched on or off by setting flags. These are the extended modeling of reverse behavior, the distributed high-frequency effects, and the increase of the avalanche current when the current density in the epilayer exceeds the doping level.

Fig.1.2 shows the equivalent circuit of Mextram model as it is specified in its latest release Level 504.12 [4]. The branches representing model currents and charges are schematically associated with different physical regions of a bipolar transistor separated by the base-emitter, base-collector, and substrate-collector junctions.

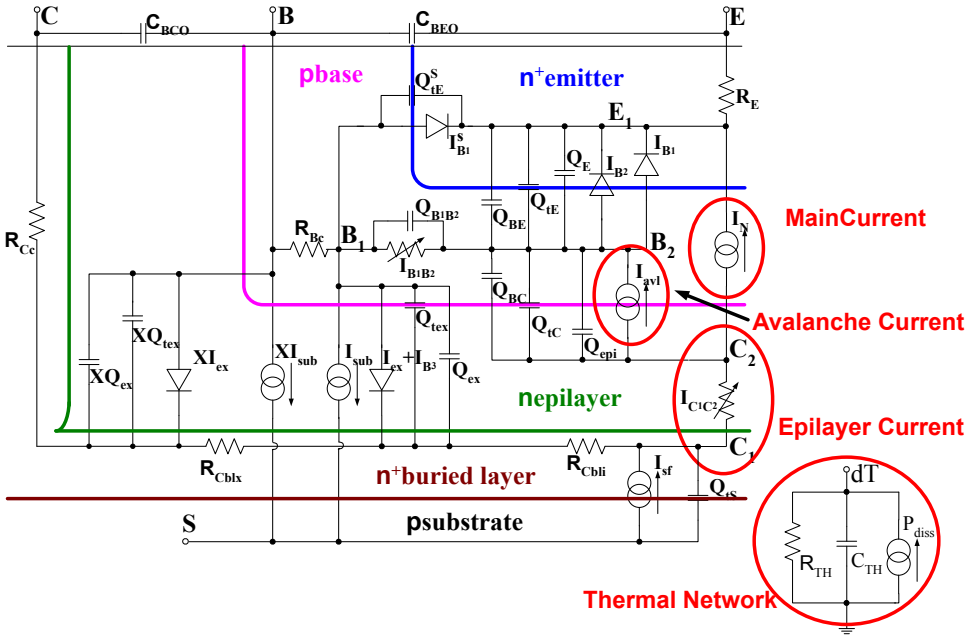

Figure 1.2: The full Mextram equivalent circuit for the vertical NPN transistor [4]

Chapter 2

Parameter extraction with circuit simulator

Since 2000, Mextram has become one of the most widely used bipolar transistor models. It is suitable for analog and digital circuit design and has demonstrated accuracy in a wide variety of applications. The accuracy of these circuit simulations not only depends on a correct mathematical description of several physical phenomena like current gain, output conductance, base push-out, cut-off frequency, noise behavior and temperature scaling, but also on a reliable robust and unambiguous transistor parameter extraction method. The use of a very sophisticated model with poorly determined parameters will result in a bad prediction of circuit performance.

2.1 Parameter extraction with ADS

Parameter extraction is a process of minimizing the difference between measurement and simulation data. And the accuracy of simulation data is crucial. The use of a very accurate compact model with poorly extracted parameters will produce bad prediction of device and circuit performance[9]. IC-CAP provides two ways of simulation: IC-CAP function package and independent circuit simulator. Compared with IC-CAP function, using simulator is much more general and user-friendly. It can work coherently and smoothly when model has been upgraded. So instead of using the simplified formulas implemented in the IC-CAP program of Agilent, in this thesis a circuit simulator called ADS (Advanced Design System) is used. ADS is an electronic design automation software for RF, microwave, and high speed digital applications. Complete, integrated set of fast, accurate and easy-to-use system, circuit and EM simulators. ADS is one product of Agilent so the software connection is simple.

2.2 Parameter extraction strategy

The general strategy of parameter extraction is to put parameters in small groups and extract these parameters simultaneously out of measured data sensitive to these parameters[8]. In the latest Mextram model, 93 parameters are given. 61 are extracted under my research work. Among these 71 parameters, 4 are Flag parameters; 38 are DC related parameters, 5 are AC related parameters, and 19 are temperature scaling related parameters. To extract parameters accurately, a specific strategy is essential. We have to think about the iteration and conflicts between parameters. To specify the order of extracted parameters in case the inaccuracy would make a chain effect. The strategy is shown in Figure 2.1

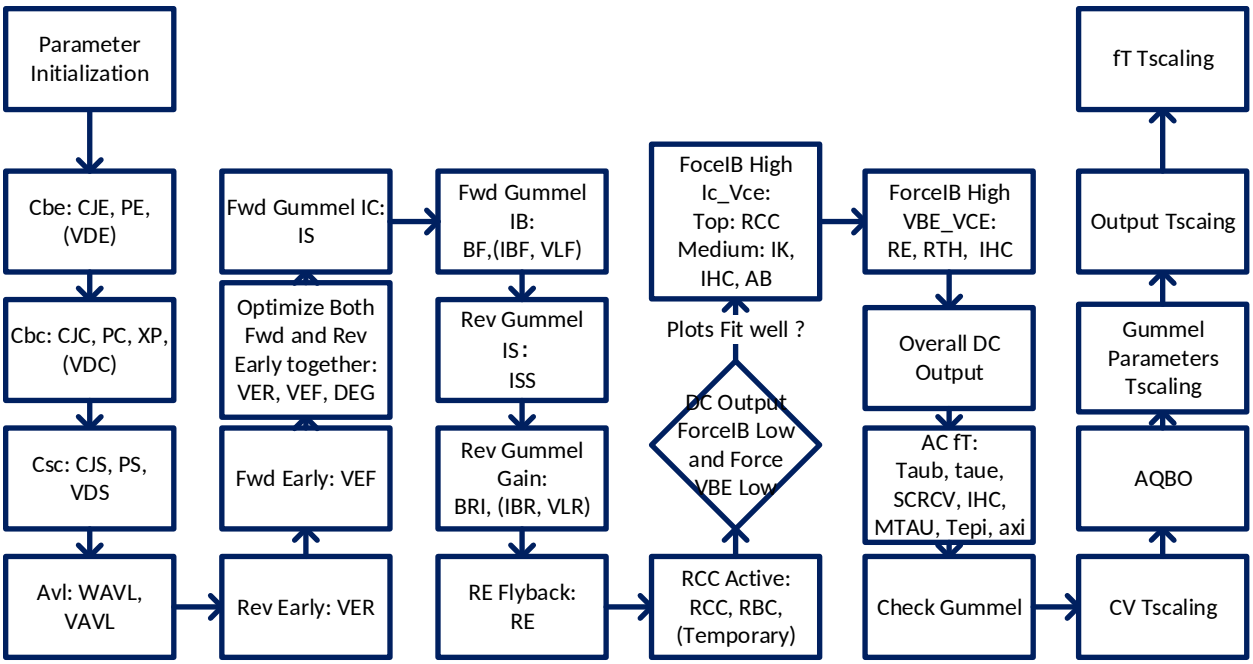

Figure 2.1: Parameter Extraction Strategy

Most of the parameters can be extracted directly from measured data, including depletion capacitance C-V, dc Gummel plots, dc output characteristics, dc Early voltage measurement, and ac S-parameter measurement. The electrical parameter extraction includes low-current parameters extraction and high-current parameters extraction. Low-current parameters extraction is straightforward. However, high-current parameters extraction is much

Base-emitter depl. cap.	C_{j_E}, p_E, (V_{d_E})
Base-collector depl. cap.	C_{j_C}, p_C, X_p
Substrate-emitter depl. cap.	C_{j_S}, p_S, (V_{d_S})
Forward-Early	W_{avl}, V_{avl}
Reverse-Early	V_{er}
Forward-Early	V_{ef}
Forward-Gummel	I_s
Forward-Gummel	β_f, I_{Bf}, m_{Lf}
Reverse-Gummel	R_E
R_{Cc}-active	R_{Cc}
Reverse-Gummel	I_{Ss}, (I_{ks})
Reverse-Gummel	β_{ri}, I_{Br}, V_{Lr}
Output-characteristic	R_{th}, I_k
Forward-Gummel	R_{Cv}, (V_{d_C})
Cut-off frequency	SCR_{Cv}, I_{hc}, τ_E, τ_{epi}, (τ_B, α_{X_i})

Table 2.1: A typical grouping of parameters in Mextram that can be used in the extraction procedure.[8]

more difficult because in that regime many physics effects play a role. In general, we first extract low-current parameters then high-current parameters, a typical sequence of the Mextram parameters extraction is given in Table 2.1.

2.3 Parameter Initialization

Parameter initialization is an essential step to start parameter extraction. Generally, parameter extraction means to minimize the difference between the measurement data and simulation data. This is done by using some algorithm that optimizes the value of the parameter. Thus, the initial value of the parameter is very important. If the initial value is good and physical, the optimizing process by IC-CAP will be accurate and efficient. Furthermore, the chance of getting stuck in a local minimum with very nonphysical values for the parameters is much smaller than stared with a random initial value.

The initial values of parameter have three types. One is given value as constant, including FLAG parameters, TYPE parameters, Model common parameters and etc. One is given based on measurements and physical general. One is needed to be calculated from layout and process data.

2.3.1 Parameters that can be given an initial value

Table 2.2 shows the parameters and their initial values. Some of them are process dependent. [8]

2.3.2 Parameters from measurements

Table 2.3 shows a list of parameters whose initial value can be obtained from measurement data and it also shows the way to get the values [8]. We can take C_{jE} and I_S as examples.

For C_{jE}, based on equation

$$C_{BE} = \frac{C_{jE}}{(1 - \frac{V_{jE}}{V_{DE}})^{p_E}} \tag{2.1}$$

It is easy to find that at zero bias condition C_{BE}=C_{jE}. So now we can take a look at Figure 2.2.

Parameter	value	remark
LEVEL	504	
T_{ref}	TEMP	The actual measurement temperature
DTA	0	T_{ref} already describes the actual temperature
EXMOD	1	Flag for extended modelling of the reverse current gain
EXPHI	1	Flag for the distrubuted high-frequency effects in transient
EXAVL	0	Flag for extended modelling of avalanche currents
EXSUB	0	Flag for extended modelling of substrate currents
m_{LF}	2	
X_{lb1}	0	
V_{Lr}	0.3	
X_{ext}	0.5	
a_{xi}	0.3	
V_{de}	0.9	Somewhat depending on process
p_E	0.4	
C_{BEO}	0.0	
C_{BCO}	0.0	
m_τ	1.0	
τ_B	-1.0	
τ_R	-1.0	
d_{Eg}	0.085	
X_{rec}	0.0	
A_{QB0}	0.3	Somewhat depending on process
A_E	0.0	Somewhat depending on process
A_B	1.0	Somewhat depending on process
A_{ex}	0.5	Somewhat depending on process
A_{epi}	2.0	Somewhat depending on process
A_C	0.5	Somewhat depending on process
$dV_{g\beta f}$	0.05	
$dV_{g\beta r}$	0.05	
V_{gB}	1.18	
V_{gC}	1.18	
V_{gj}	1.18	
$dV_{g\tau e}$	0.0	
V_{ds}	0.6	Somewhat depending on process
p_S	0.3	
V_{gs}	1.18	
A_S	2.0	Somewhat depending on process
R_{th}	2.5k	

Table 2.2: Parameter initial value [8]

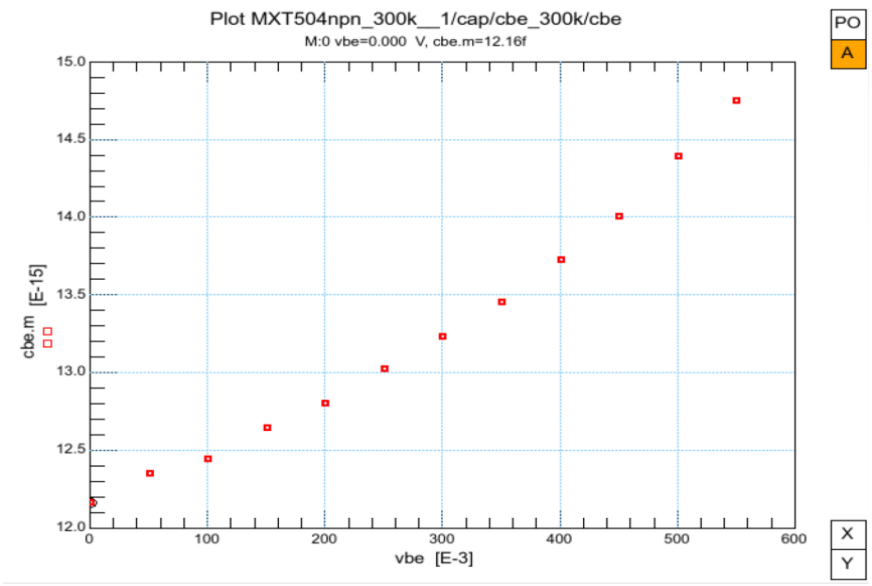

Figure 2.2: Base emitter capacitance measurement data.

From the measurement we can estimate the initialization of C_{jE} as 12.16f. C_{jC} and C_{jS} use the similar approach to estimate the initialization value.

For the initialization of I_S we can use function 3.19.

$$I_C = \frac{I_S\, e^{V_{BE}/V_T}}{q_I}, \tag{2.2}$$

At zero bias V_{BE}=0, then I_C=I_S. From Figure 2.3 we can estimate the initial value of I_S as 5e-18.

The initialization estimate strategy is also listed in table2.3.

2.3.3 Parameters to be calculated

At last, we have same parameters whose initial value need to be calculated from laylout and process data. We also need following constant to get the initial values.

Boltzmann constant is :

$$k = 1.3806226 \times 10^{-23}\,\mathrm{JK}^{-1}, \tag{2.3}$$

Param	Way of extraction
C_{jE}	Zero bias values of base-emitter capacitance
C_{jC}	Zero bias values of base-collector capacitance
C_{jS}	Zero bias values of substrate-collector capacitance
R_E	Numerical derivative in R_E-flyback measurement
V_{er}	Numerical derivative in reverse-Early measurement
V_{ef}	Numerical derivative in forward-Early measurement
β_f	Maximum of forward current gain
β_{ri}	Maximum of internal reverse current gain
I_S	From forward-gummel collector current without Early effect
I_{Ss}	From reverse-gummel substrate current without Early effect
τ_E, τ_B	$1/[10\ \pi\ \max(f_T)]$

Table 2.3: Parameters that can be estimated from measurement [8].

MULT	Numbers of transistors in parallel
H_{em}	Emitter width(Dimension on silicon)
L_{em}	Emitter strip length(dimension on silicon)
ρ_p	Pinched sheet resistance of the base
N_{base}	Number of base stripes
N_{epi}	Collector epilayer doping level
W_{epi}	Collector epilayer thickness

Table 2.4: The layout and process quantities [8].

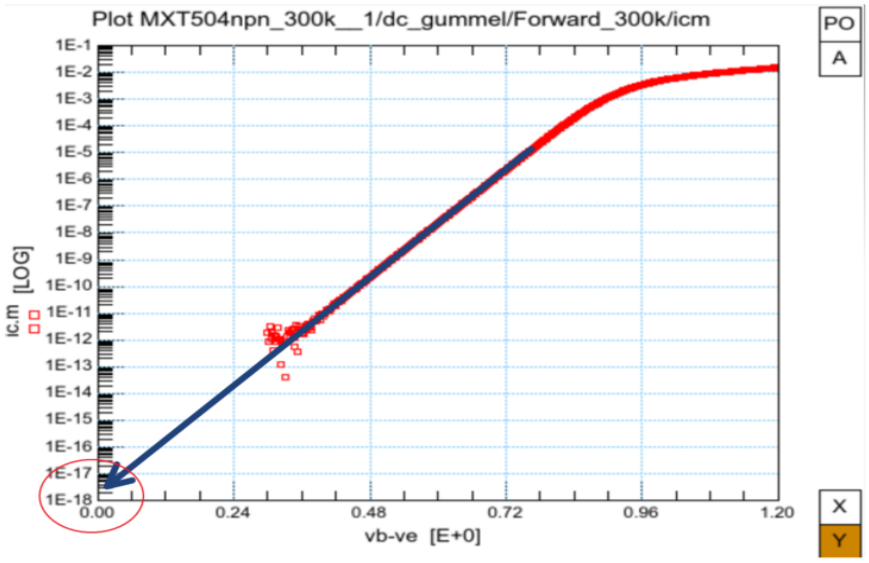

Figure 2.3: Collector current measurement data.

The elementary charge is :

$$q = 1.6021918 \times 10^{-19}\,\mathrm{C}, \tag{2.4}$$

Dielectric constant is shown as:

$$\varepsilon = 1.036 \times 10^{-10}\,\mathrm{C/Vm}, \tag{2.5}$$

The saturated drift velocity is:

$$v_{sat} = 8.0 \cdot 10^{4}\,\mathrm{m/s}. \tag{2.6}$$

Process quanties are emitter width:

$$H_{em} = 0.5\mu m, \tag{2.7}$$

emitter stripe length:

$$L_{em} = 2.5\mu m, \tag{2.8}$$

base doping:

$$N_{base} = 1 \times 18cm^{-3}, \tag{2.9}$$

epilayer doping:

$$N_{epi} = 3 \times 17cm^{-3}, \tag{2.10}$$

From layout data we can calculate the emitter surface(A_{em}) and periphery(P_{em})

$$A_{em} = H_{em} \cdot Lem, \tag{2.11}$$

$$P_{em} = 2(H_{em} + L_{em}). \tag{2.12}$$

From the layout data and direct extraction estimates we can calculate the fraction of the BE depletion capacitance $XC_{jE}$and the fraction of the BC depletion capacitance XC_{jC}

$$XC_{jE} = \frac{P_{em}}{P_{em} + 6A_{em}/\mu m}, \tag{2.13}$$

$$XC_{jC} = XC_{jE}\frac{V_{er} \cdot C_{jE}}{V_{ef} \cdot C_{jC}}. \tag{2.14}$$

Here C_{jE} is zero-bias emitter-base depletion capacitance; C_{jC} is zero-bias collector-base capacitance; V_{er} is reverse early voltage; V_{ef} is forward early voltage.

The zero bias value of the variable base resistance R_{Bv} and the constant part of the base resistance R_{Bc} can be estimated as

$$R_{Bv} = \frac{H_{em}\rho_p}{3N_{base}^2 L_{em}} \tag{2.15}$$

$$R_{Bc} = R_{Cc} = \frac{300\Omega\mu m}{L_{em}} \tag{2.16}$$

The initial values of the collector-emitter high injection knee current I_K and base-substrate high injection knee current I_{kS} are

$$I_K = \frac{V_{er}(1 - XC_{je})C_{je}}{\tau_B}, \tag{2.17}$$

$$I_{kS} = (500\mu A/\mu m^2) \times A_{em}. \tag{2.18}$$

$$\tag{2.19}$$

τ_B is transit time of stored base charge.

The initial values of saturation current of the non-ideal reverse base current I_{Br} and saturation current of the non-ideal forward base current I_{Bf}

$$I_{Br} = 100I_S, \tag{2.20}$$

$$I_{Bf} = 100I_S. \tag{2.21}$$

The epilayer thickness (W_{epi}) used in weak-avalanche model W_{avl} and voltage determining curvature of avalanche current V_{avl} calculation:

$$W_{avl} = W_{epi}, \tag{2.22}$$

$$V_{avl} = \frac{qN_{epi}W_{epi}^2}{2\varepsilon}. \tag{2.23}$$

We also need some spreading parameters for the epilayer: α_l is the spreading angle at low current levels($I_C < I_{hc}$) while α_h is the spreading angle at high current levels. These quantities are process and geometry dependent. We can use the following values if we are

only interested in generating an initial parameters set:

$$\tan \alpha_{\mathrm{l}} = 0.5, \tag{2.24}$$

$$\tan \alpha_{\mathrm{h}} = 1.0, \tag{2.25}$$

$$S_{Fl} = \tan \alpha_{\mathrm{l}} \mathrm{W_{epi}} (\frac{1}{\mathrm{H_{em}}} + \frac{1}{\mathrm{L_{em}}}), \tag{2.26}$$

$$S_{Fh} = \frac{2}{3} \tan \alpha_{\mathrm{h}} \mathrm{W_{epi}} (\frac{1}{\mathrm{H_{em}}} + \frac{1}{\mathrm{L_{em}}}). \tag{2.27}$$

The latter quantity is the current spreading factor for high injection, and is a parameter used in the high-current avalanche model. We can now calculate the epilayer parameters. The collector-base diffusion voltage:

$$V_{dc} = V_T ln(N_{epi}^2 / n_i^2), \tag{2.28}$$

Resistance of the un-modulated epilayer is :

$$R_{Cv} = \frac{W_{epi}}{q \mu_0 N_{epi} A_{em}} \frac{1}{(1 + S_{Fl})^2}, \tag{2.29}$$

Critical current for velocity saturation in the epilayer can be estimated as :

$$I_{hc} = q \mu_0 N_{epi} A_{em} v_{sat} (1 + S_{Fl})^2, \tag{2.30}$$

The initial value of space charge resistance of the epilayer is :

$$SCR_{Cv} = \frac{W_{epi}^2}{2 \varepsilon v_{saat} A_{em}} \frac{1}{(1 + S_{Fl})^2}, \tag{2.31}$$

The constant part of C_{jC}, collector-base grading coefficient, coefficient for the current modulation of the collector-base depletion capacitance are:

$$X_p = xd_0/W_{epi}, \tag{2.32}$$

$$p_C = 0.3/(1 - X_p), \tag{2.33}$$

$$m_C = (1 - X_p)/2, \tag{2.34}$$

The transit time of stored epilayer charge and transit time of reverse extrinsic stored base charge are:

$$\tau_{epi} = \frac{W_{epi}^2}{4\mu_0 V_T} \tag{2.35}$$

$$\tau_R = (\tau_B + \tau_{epi}\frac{1 - XC_{jc}}{XC_{jc}}). \tag{2.36}$$

Chapter 3

Extraction of DC Parameters at 300K

Since almost all parameter have temperature scaling effect, we need to extract one set of parameters in one temperature and set it as reference temperature. Generally we will set it at room temperature 25 $°C$ or 26.85 $°C$ (which equals 300K).

3.1 Capacitance

Capacitance contains a few important basic parameters which are essential for later parameter calculation so it is the first step of this extraction. Since capacitance values can not be calculated by simulator then generally depletion capacitance parameters can be extracted using simulators when Y-parameters and S-parameters measurement data is given. However, for this set of measurement data, Y-parameters and S-parameters are not given during depletion capacitance measurement, IC-CAP functions are used for all C-V parameter extraction process.

3.1.1 Base-emitter depletion capacitance

The measurement C_{BE} is consisted by three parts: depletion capacitance, overlap capacitance and diffusion capacitance.The depletion capacitance and overlap capacitance dominate as long as V_{BE} bias is not too high. As there is no currents flowing then no voltage drop over resistors occur under this circumstance. So capacitance can be approximated by the almost ideal formula:

$$C_{BE} = \frac{C_{jE}}{(1 - \frac{V_{jE}}{V_{DE}})^{p_E}}, \tag{3.1}$$

$$V_{jE} = V_{BE} - 0.1V_{dE} \ln(1 + e^{\frac{V_{BE} - V_{FE}}{0.1V_{dE}}}), \tag{3.2}$$

$$V_{FE} = V_{dE}(1 - a_{jE}^{-\frac{1}{PE}}), \tag{3.3}$$

C_{j_E} is the zero-bias emitter base depletion capacitance, V_{d_E} is diffusion voltage and p_E describes emitter-base grading coefficient. a_{jE} is a constant 3 here. However, C_{BEO} which describes the overlap capacitance between base and emitter should be considered as a part of C_{be}. But due to lack of information we can not set the value of C_{BEO}. Se we set the C_{BEO} zero.

Using IC-CAP function MXT_cbe, we could get calculation data cbe_s. From plot $C_{BE} - V_{BE}$ by fitting measurement data cbe.m and calculation data cbe_s, C_{j_E} , p_E and V_{d_E} can be extracted. The extraction result is shown in Figure 3.1.

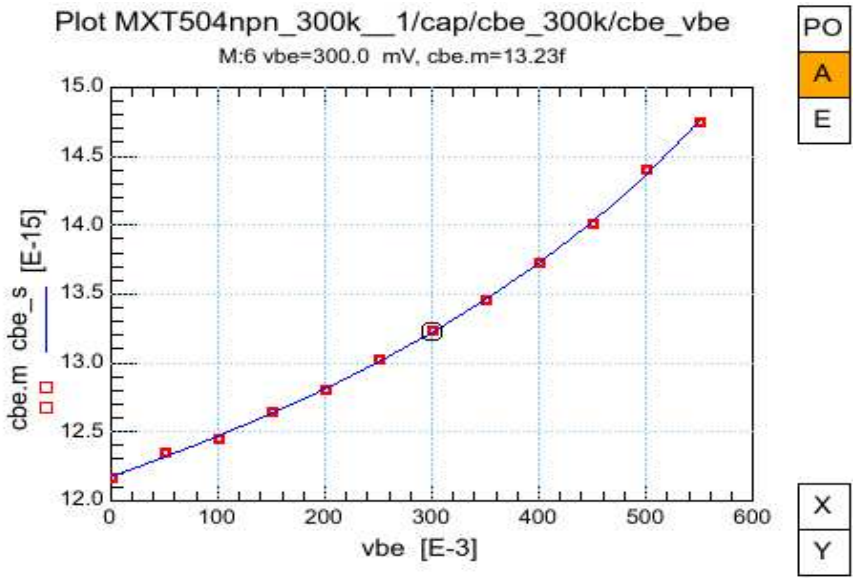

Figure 3.1: Measured(markers) and calculated(line) base emitter depletion capacitance

3.1.2 collector depletion capacitance

The extraction of the base-collector depletion capacitance is close to the base- emitter depletion capacitance. The base-collector depletion capacitance can be written as:

$$C_{BC} = \frac{S_C(1-X_p)C_{jC}}{(1-V_{jC}/V_{dC})^{p_C}} + \frac{(1-S_C)(1-X_p)C_{jC}}{(1-V_{FC}/V_{dC})^{p_C}} + X_P C_{jC}, \tag{3.4}$$

$$V_{jC} = V_{BC} + 0.1V_{dC}\ln(1/(1+e^{\frac{V_{BC}-V_{FC}}{0.1V_{dC}}}), \tag{3.5}$$

$$V_{FC} = V_{dC}(1-(\frac{a_{jC}-X_P}{1-X_P})^{-\frac{1}{p_C}}), \tag{3.6}$$

$$S_C = \frac{1}{1+e^{\frac{V_{BC}-V_{FC}}{0.1V_{dC}}}} \tag{3.7}$$

We have $a_{jC} = 2$ here. Parameter X_P is introduced to describe the finite thickness of collector epilayer.The constant capacitance C_{BCO} which describes base-collector overlap capacitance is set to zero. C_{jC} describes zero bias collector-base depletion capacitance, p_C is collector-base grading coefficient, V_{dC} is collector-base built-in voltage. The extraction strategy is also very simple. Using IC-CAP function MXT_cj0 to get C_{jC} which gives extraction a better initial value. And with IC-CAP function MXT_cbc and given numbers of TEMP and CJC, we can extract C_{jC}, p_C, and X_P by fitting the $C_{BC} - V_{BC}$ curve as shown in Figure 3.2.

Help parameter V_{dC} will be re-extracted when we need to fit the high injection region of forward current gain, because it has strong impact on the current gain roll-off, cut-off frequency roll-off and output characteristics quasi-saturation region. This iteration will happen repeatedly during extraction process because many parameters are used in several equations. We need to make sure the whole set parameter can fit most of simulations instead of getting one good mathematical result that only fits one specific plot.

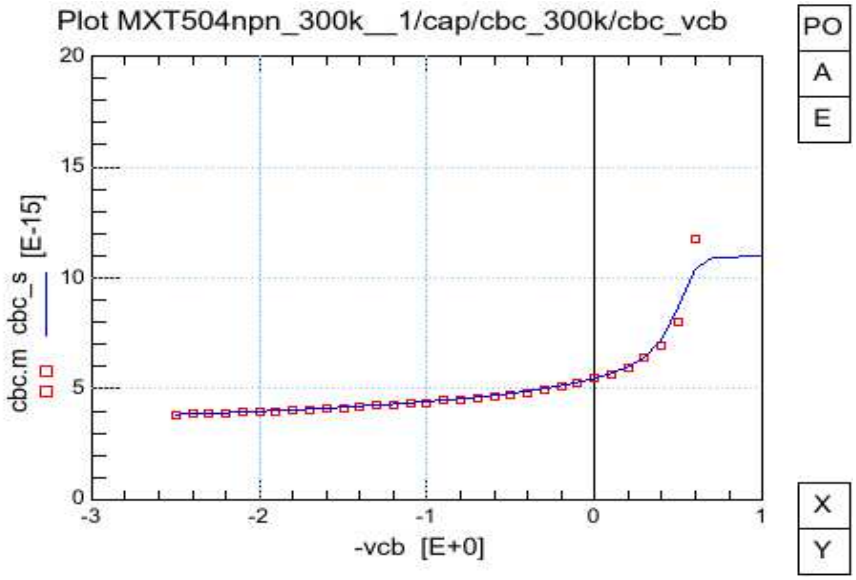

Figure 3.2: Measured(markers) and calculated(line) base collector depletion capacitance

3.1.3 Collector-substrate depletion capacitance

The extraction of collector-substrate capacitance is also very similar. The collector-substrate depletion capacitance can be written as :

$$C_{SC} = \frac{C_{jS}}{(1 - \frac{V_{jS}}{V_{DS}})^{p_S}}, \tag{3.8}$$

$$V_{jS} = V_{SC} - 0.1V_{dE} \ln(1 + e^{\frac{V_{SC} - V_{FS}}{0.1V_{dS}}}), \tag{3.9}$$

$$V_{FS} = V_{dE}(1 - a_{jS}^{-\frac{1}{PS}})' \tag{3.10}$$

C_{jS} describes zero bias collector-substrate depletion capacitance which we can use ICCAP function MXT_cj0 to extract. p_S is collector-substrate grading coefficient. V_{dS} is collector-substrate diffusion voltage. It is difficult to extract directly. However, it is not used in any other part of the model so the combination extraction will not be a big problem.

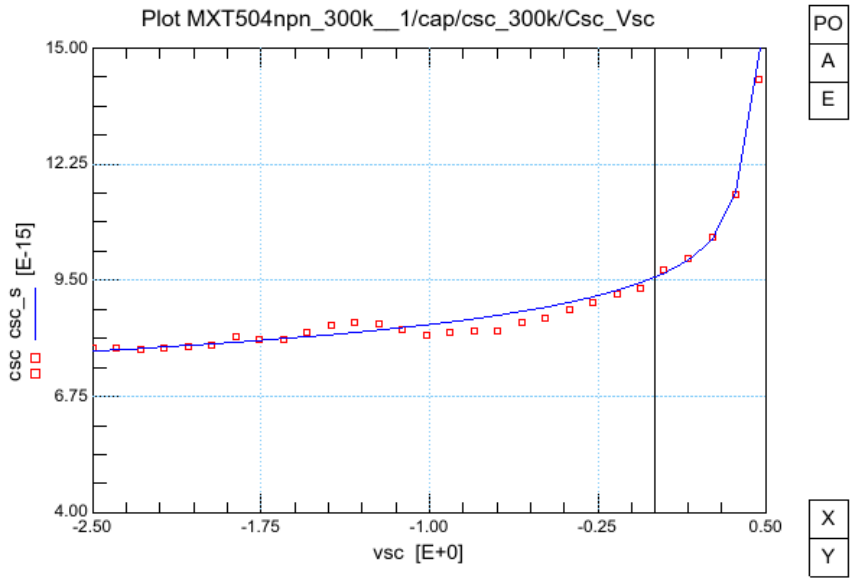

Figure 3.3: Measured(markers) and calculated(line) substrate collector depletion capacitance

With IC-CAP function MXT_csc , the calculated data csc_s is plotted. By fitting csc.m with csc_s plots, C_{jS} and p_S can be extracted. Figure 3.3 show the extracted $C_{SC} - V_{SC}$ result.

3.2 Avalanche

In modern transistor because we have low breakdown voltage we cannot neglect avalanche effect. The avalanche current is a result of impact ionization in the epilayer due to the high electric fields. This generation of avalanche currents strongly depends on the maximum electric field. The low current avalanche parameters are extracted from base current under forward-early measurement shown in Figure 3.4.

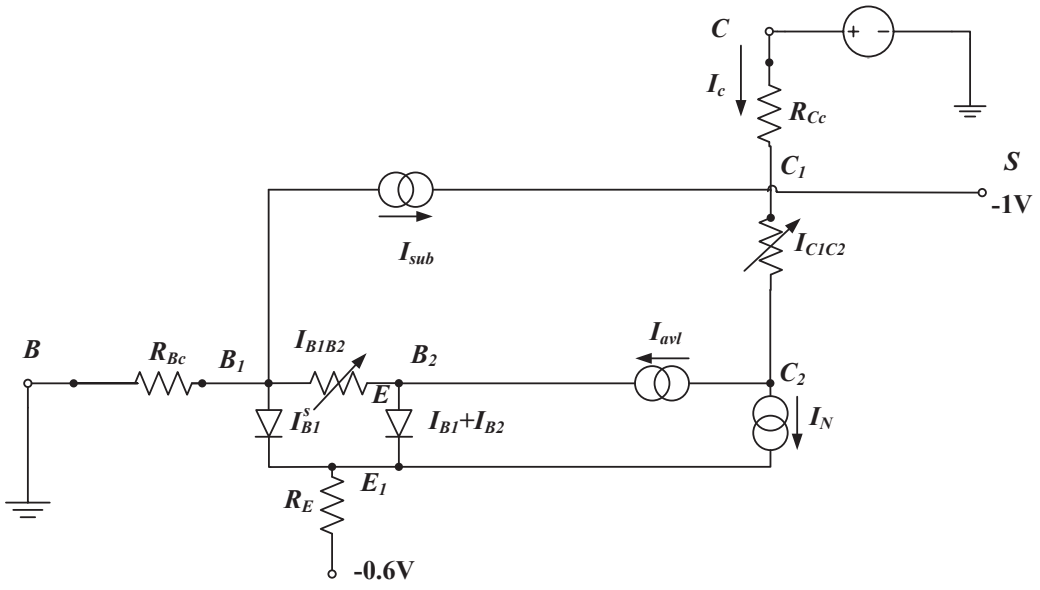

Figure 3.4: Forward-Early measurement simplified circuit [5]

Because of avalanche current the base current will drop down as the increase of V_{CB}. So that the avalanche current can be written as:

$$I_{avl} = I_{B0} - I_B. \tag{3.11}$$

Here I_{B0} is the current that shows the base current at $V_{CB} = 0$ .The avalanche current can also be described as:

$$I_{avl} = I_C, noavl\, G_{EM}, \tag{3.12}$$

G_{EM} is the generation factor:

$$G_{EM} = \frac{A_n}{B_n} E_M \lambda_D \{exp[\frac{-B_n}{E_M}] - exp[-\frac{B_n}{E_M}(1 + \frac{W_{avl}}{\lambda_D})]\}, \tag{3.13}$$

$$\lambda_D = \frac{W_{avl}^2}{2V_{avl}} E_M, \tag{3.14}$$

$$E_M = \frac{V_{d_C} + V_{CB} + 2\,V_{avl}}{W_{avl}} \sqrt{\frac{V_{d_C} + V_{CB}}{V_{d_C} + V_{CB} + V_{avl}}}. \tag{3.15}$$

A_n and B_n are material constants, which are avalanche coefficient. λ_D is the extrapolated depletion thickness where the electric field is zero, effective width of the epilayer for avalanche current W_{AVL} and voltage describing the curvature of the avalanche current V_{AVL} are parameters we need to extract here. From these equations we can see that the G_{EM} factor is a coefficient that is related to V_{CB}, W_{AVL} and V_{AVL}. So now we need to find this coefficient, then fitting the simulation data to measurement data can help extract the parameters we need.

However, when taking a look at this measurement circuit, it is obvious that the measurement I_C contains avalanche current part. So this means that measurement I_C and I_B data are not the same as the simulation came from ADS simulator through Mextram model verilogA code. The difference is shown from Figure 3.5 to Figure 3.6.

Thus we need to use a program to calculated the measurement data to give the plot we actually need. Since we use ADS to generate the simulation data, I write a program and put it through this circuit simulator. And here is program code:

```
Gem:


Ib0m=ib.m[0]
Ib0s=ib.s[0]
!print "Ib0m="; Ib0m  ; "Ib0s=" ;   Ib0s
ibdelta=ib
i=0
```

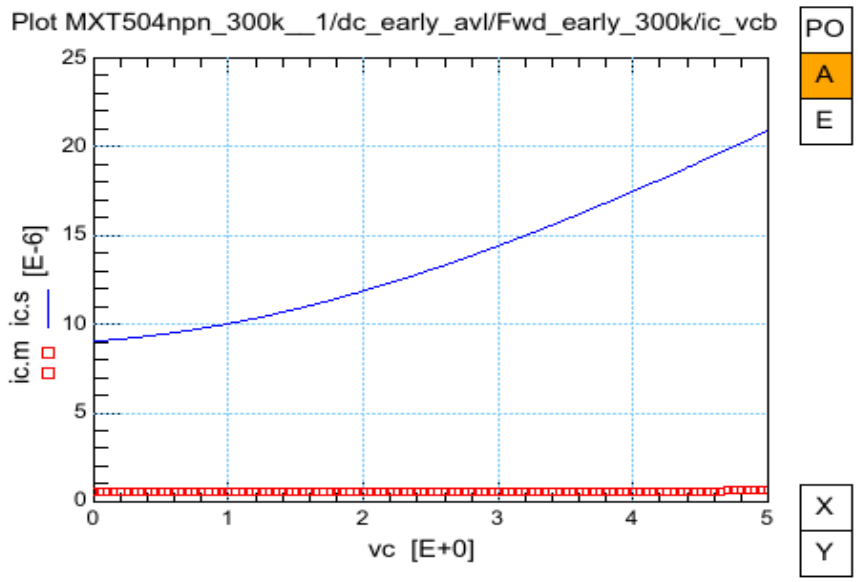

Figure 3.5: Measured(markers) and simulated(line) Measured and Simulated Collector Current Comparasion without Program calculated

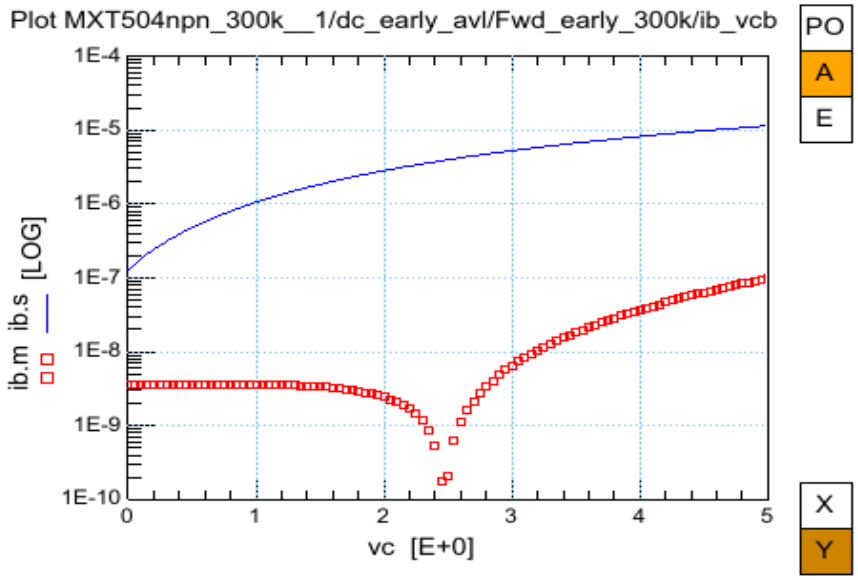

Figure 3.6: Measured(markers) and simulated(line) Measured and Simulated Base Current Comparasion without Program calculated

```
while i<size(vc)
ibdelta.m[i]=Ib0m-ib.m[i]
ibdelta.s[i]=Ib0s-ib.s[i]
i=i+1
end while
mydata=ic
q=0
while q<size(vc)
mydata.m[q]=ibdelta.m[q]//(ic.m[q]-ibdelta.m[q])
mydata.s[q]=ibdelta.s[q]//(ic.s[q]-ibdelta.s[q])
q=q+1
end while
return mydata + 1e-6
```

After this program, we optimize the measurement and simulation result. As the collector-base bias gets larger, the base current drops below zero because of the avalanche effect. The extraction result is shown in Figure 3.7 - Figure 3.8 .

3.3 Early Effect

The Early effect, named after its discoverer James M. Early, is the variation in the width of the base in a BJT due to a variation in the applied base-to-collector voltage. A greater reverse bias across the collector base junction, for example, increases the collector base depletion width, decreasing the width of the charge carrier portion of the base. Under increased collector base reverse bias, a widening of the depletion region in the base and the associated narrowing of the neutral base region will happen. The collector depletion region also increases under reverse bias, more than does that of the base, because the collector is less heavily doped. The principle governing these two widths is charge neutrality. The narrowing of the collector does not have a significant effect as the collector is much longer than the base. The emitter base junction is unchanged because the emitter base voltage is the same.

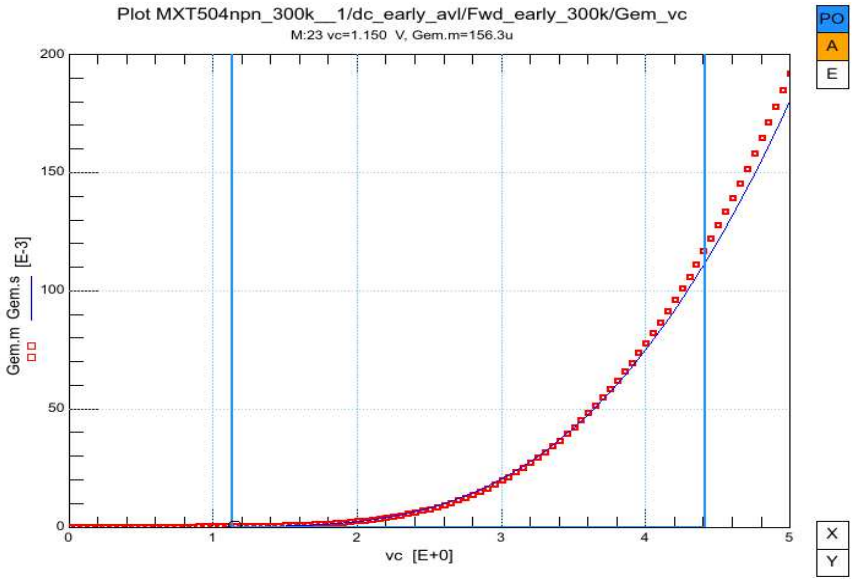

Figure 3.7: Measured(markers) and simulated(line) Gem

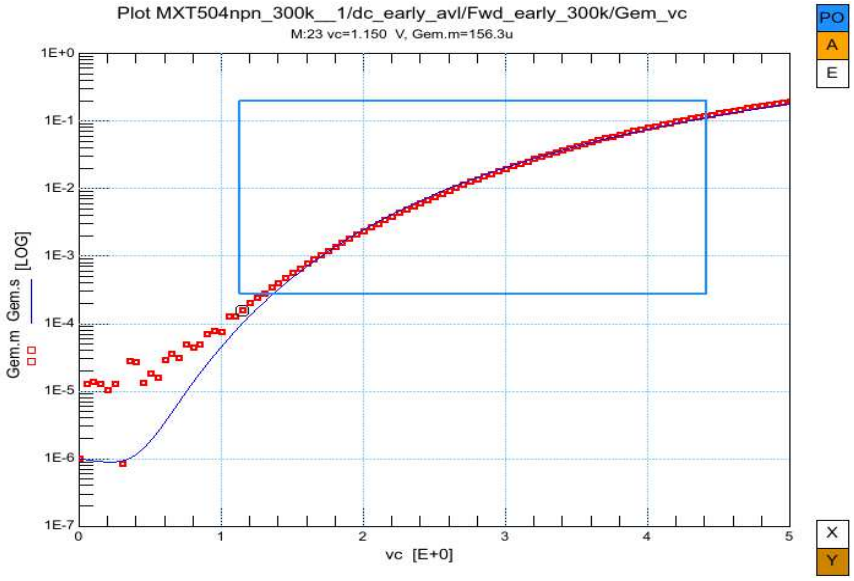

Figure 3.8: Measured(markers) and simulated(line) Gem Logscale

In Mextram we have two parameters V_{er} and V_{ef} to describe Early effect. Mextram is a SiGe transistors. Since the Ge concentration has a non-zero slope, Mextram redefine a coefficient q_0^I to describe Early effect for the currents.

$$q0I = \frac{exp([\frac{V_{tE}}{V_{erT}} + 1]\frac{DEG_T}{VT}) - exp[(\frac{-V_{tC}}{V_{efT}}\frac{DEG_T}{VT})}{exp(\frac{DEG_T}{VT}) - 1}, \tag{3.16}$$

DEG is the difference of the bandgap over the neutral base. In Mextram DEG is also an important parameter for Early Effect. Since V_{er}, V_{ef}, and DEG are all used in both Reverse Early Voltage and Forward Early Voltage calculation, I used programs to calculate two factors, FreVearly and Fearly, in Reverse Environment and Forward Early Environment. Then use plot optimizer to fit both programs together by optimizing DEG, V_{er}, and V_{ef} together.

$$FreVearly = \frac{I_E}{I_{E0}}, \tag{3.17}$$

$$Fearly = \frac{I_C - (I_{B0} - I_B)}{I_{C0}}, \tag{3.18}$$

Here I_{E0} stands for the emitter current at V_{BE}=0 during reverse bias; I_{C0} stands for the collector at V_{CB}=0 at forward bias. When the optimization is running, the number could be varied since it is a mathematical process. The optimized parameter values could help the plots fitting well but they are not reasonable. So the range setting is very important. We need to make sure is parameter is extracted around a reasonable and physical number. In this case we need to set DEG range between 35m to 85m to make sure it is realistic and physically reasonable. V_{ef}, V_{er}, DEG extraction result is shown in Figure 3.9 - 3.10.

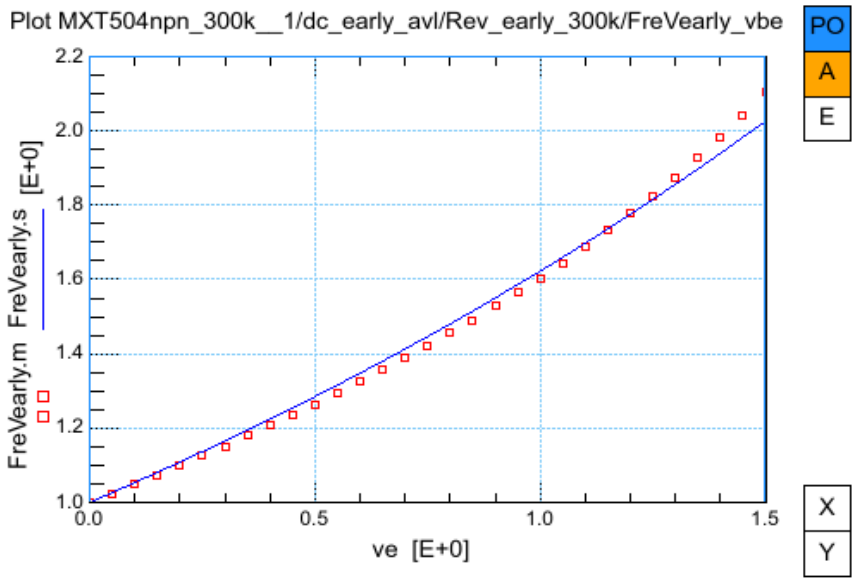

Figure 3.9: Measured(markers) and simulated(line) Reverse Early Voltage coefficent FreVearly

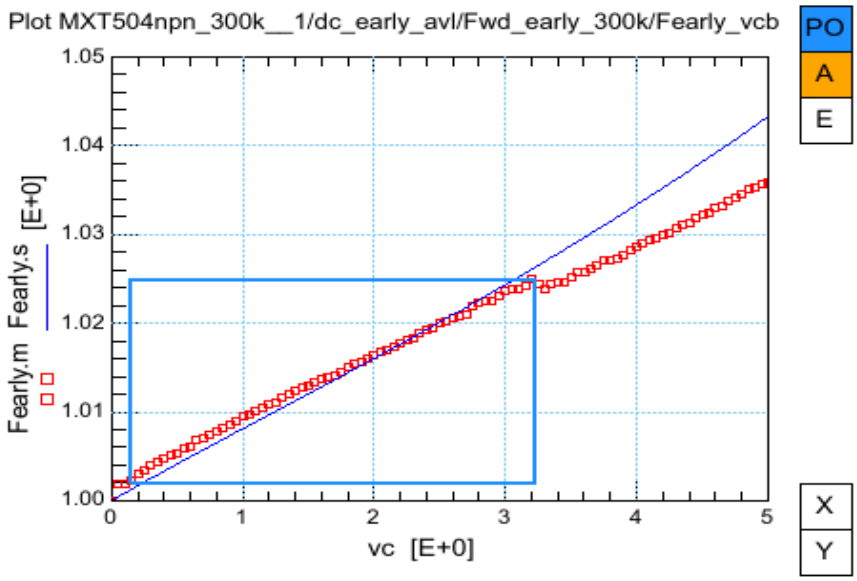

Figure 3.10: Measured(markers) and simulated(line) Forward Early Voltage coefficent Fearly

3.4 DC Gummel

3.4.1 Collector saturation current

Since we have a good description of Early effect, we can extract the collector saturation current in forward-Gummel measurement(shown in Figure 3.11) at low base-emitter bias.

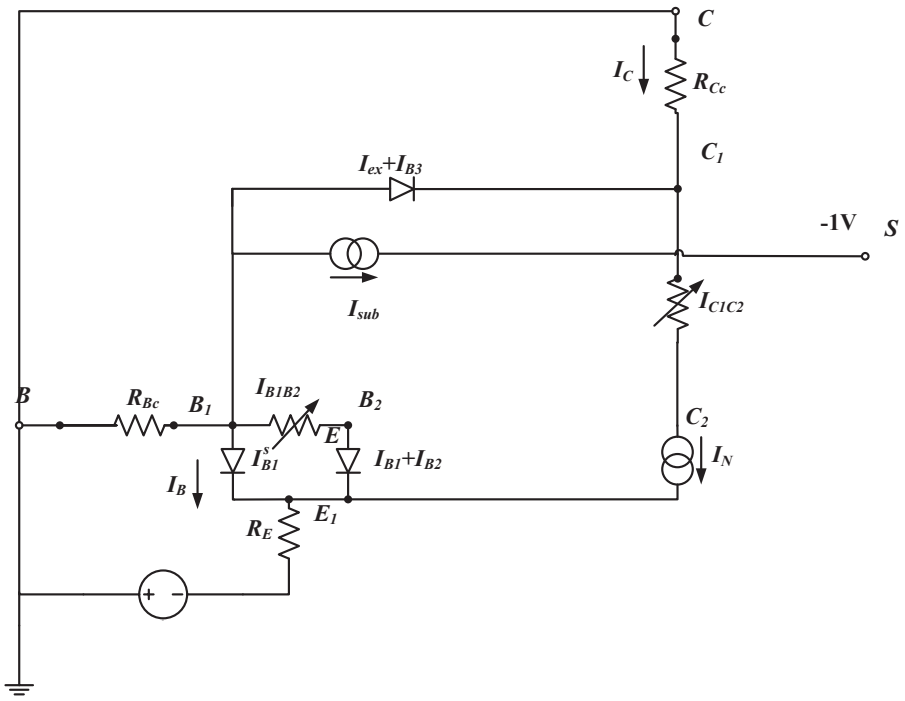

Figure 3.11: Forward-Gummel measurement simplified circuit [5]

The collector current I_C is proportional to the increase of base-emitter bias at low bias. At high bias the resistance effect can not be neglected and the actual V_{B_2E1} will be much less than V_{BE} we used , which is the reason that measurement data and simulation data is split in high bias. So we will only focus on the low bias behavior and optimize data at low bias area.

$$I_C = \frac{I_S\, e^{V_{BE}/V_T}}{q_I}, \tag{3.19}$$

Here V_T is the thermal voltage, which needs to be determined accurately from the actual absolute temperature. q_I is a factor that is related to V_{er}, V_{ef}, DEG, PE, VDE, VDC,

PC, and XP. From former extraction process we already have good trustworthy values of these parameters. Then by fitting I_C we can extract a good value of parameter IS. The extraction result is shown in Figure 3.12.

The optimization range between 0.58V to 0.9V is needed. When the vbc is too low, the measurement is not accurate; when voltage is higher than 0.9V, the q_I factor will not be the only part in Ic calculation. More high injection effect parameters need to be put in thought. So try to make sure the extraction accurate, we need to set the optimization range in this reasonable range.

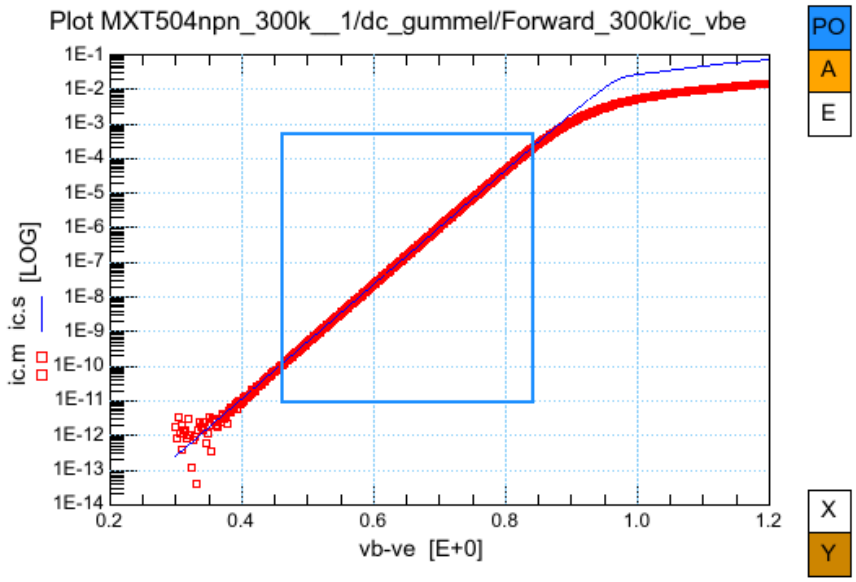

Figure 3.12: Measured(markers) and simulated (line) collector current in forward-Gummel measurement

3.4.2 Forward base current

From last section, collector current is already fitted in reasonable range. Thus for forward base current parameter can be extracted from fitting just base current in forward-Gummel measurements (shown in Figure 3.11) by comparing the measurement forward base current and simulated forward base current.

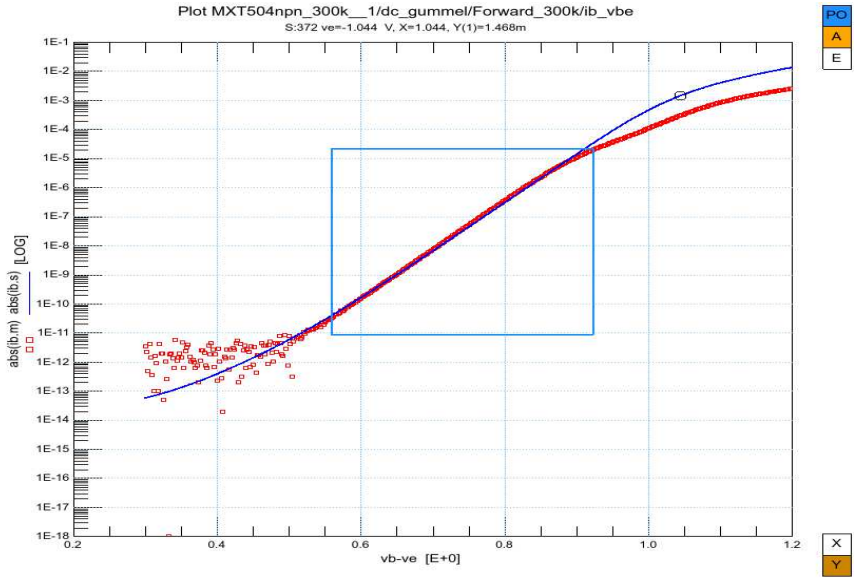

Figure 3.13: Measured(markers) and simulated(line) base current in forward-Gummel measurement [5]

As we take the internal bias equal to the external bias V_{BE}, we must make sure that resistance effects are not important so we need to fit the curve at low base-emitter bias.

The ideal and non-ideal base current can be described as below:

$$I_{B1} = \frac{I_S}{\beta_f} e^{V_{B_2E_1}/V_T}, \tag{3.20a}$$

$$I_{B2} = I_{Bf}\left(e^{V_{B_2E_1}/m_{Lf}V_T} - 1\right) + G_{min}(V_{BE} + V_{BC}), \tag{3.20b}$$

$$I_B = I_{B1} + I_{B2}, \tag{3.20c}$$

Here ideal forward current gain β_f, saturation current of the non ideal forward base current I_{Bf} and none-ideality factor of the non-ideal forward base current m_{Lf} are used.

β_f, I_{Bf} and m_{Lf} are extracted here from the comparison of simulated forward base current and the measurement forward base current shown in Figure 3.13.

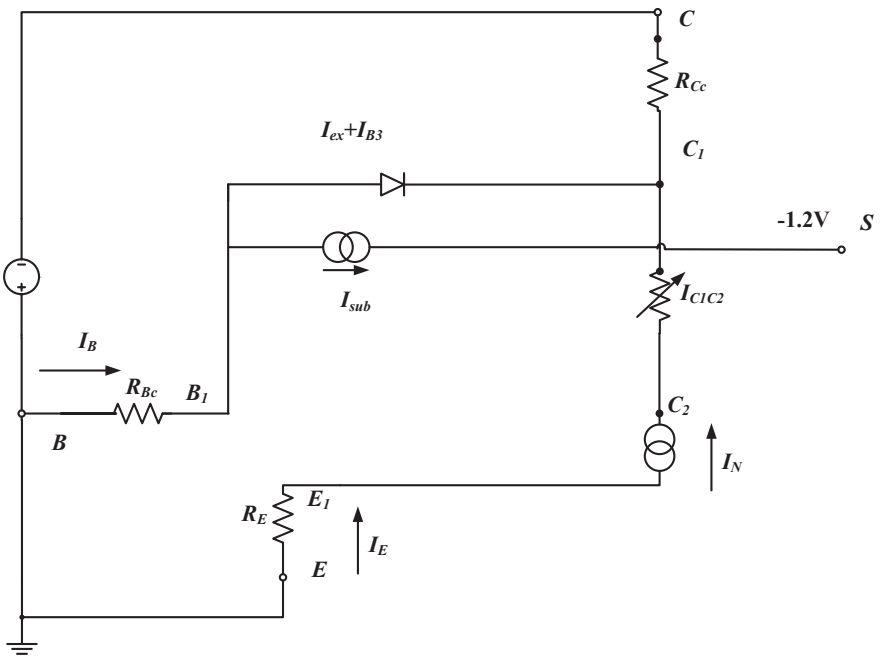

Figure 3.14: Reverse-Gummel measurement simplified circuit [5]

3.4.3 Substrate saturation current

The substrate saturation current is extracted in reverse-Gummel measurement as shown in Figure 3.14 by fitting the substrate current I_{sub} . We will neglect the voltage drop and the substrate current can be calculated by equation:

$$I_{sub} = I_{Ss} \exp(\frac{V_{BC}}{V_T}), \tag{3.21}$$

I_{Ss} can be extracted directly from the substrate current. The extraction result is given in Figure 3.15. At high bias, because of the voltage drop over R_{Cc}, $V_{B_1C_1}$ will be less than V_{BC}, so that measured and simulated substrate current can not be fit yet at high base-collector bias.

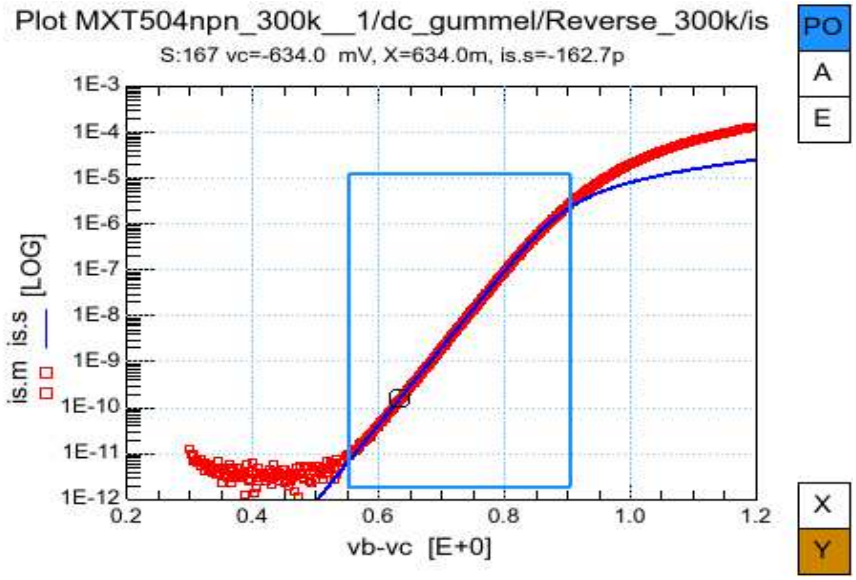

Figure 3.15: Measured(markers) and simulated(line) substrate current in reverse Gummel

3.4.4 Reverse current gain

The reverse current gain parameters are extracted from reverse-Gummel measurement. In the reverse-Gummel measurement (shown in Figure 3.11) the base-collector is forward biased which means the external base current contains internal base current and substrate current.

$$hfc = \frac{I_E}{I_B - I_{sub}}, \tag{3.22}$$

$$I_B - I_S = \frac{I_s}{BRI} e^{\frac{V_{b1c1}}{VT}} + IBR \frac{e^{\frac{V_{b1c1}}{VT}}}{e^{\frac{V_{b1c1}}{2VT}} + e^{\frac{VLR}{2VT}}} + G_{min}(V_{BE} + V_{BC}), \tag{3.23}$$

Based on these equations, we can write a program of $bsub$=I_B-I_{sub}. And then return:

$$hfc = \frac{I_C}{I_B - I_{sub}}, \tag{3.24}$$

The reverse current gain β_{ri}, saturation current of the non-ideal reverse base current I_{BR} and cross-over voltage of the non-ideal reverse base current V_{Lr} are variable of I_B-I_{sub}. So that they can be extracted by fitting the curve. Again we need only concentrate on the low base-collector bias. Because before high injection we could approximiately see input voltage as V_{b1c1} then we can use this function to extract β_{ri}, I_{BR}, and V_{Lr}. As the same problem in forward current gain extraction, we can extract β_{ri} accurately in the ideal region, which is the box in Figure 3.17.

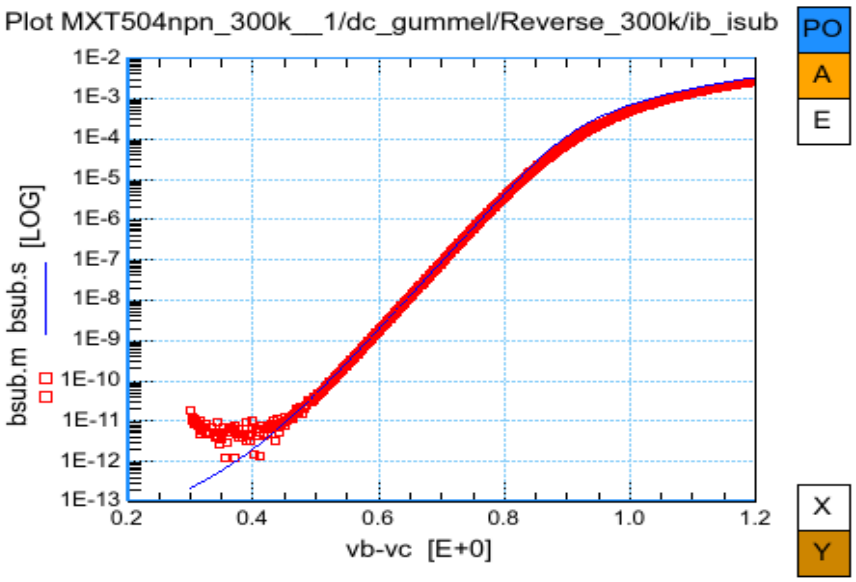

Figure 3.16: Measured(markers) and simulated(line) I_B-I_{sub} plot

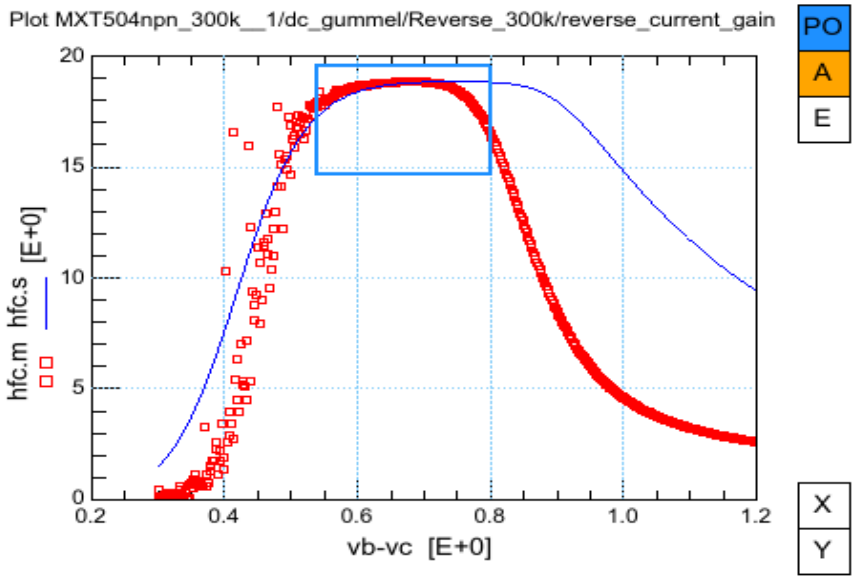

Figure 3.17: Measured(markers) and simulated(line) reverse current gain

3.5 Resistor Initial Estimation

3.5.1 R_E Flyback

One of the simplest way to extract the emitter resistance is from the Giacoletto method [?] [?]. The collector current is kept zero and the V_{BE} is increased . The collector-emitter saturation voltage can be estimated as $V_{CES} \approx I_E R_E$. Then the emitter resistance can be obtained by taking the derivative of V_{CES} with regard to I_E:

$$R_E = \frac{\partial V_{CES}}{\partial I_E}. \tag{3.25}$$

So a very simple way is to plot out the V_{CE}-I_E and to fit the slope of two curves by optimizing the value of R_E. The result is shown in Figure 3.18.

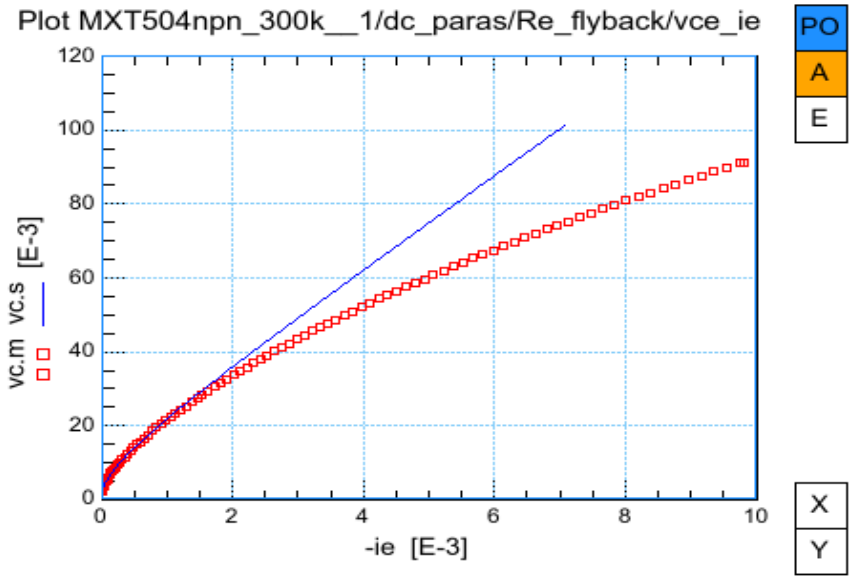

Figure 3.18: Measured(markers) and simulated(line) R_E flyback measurement.

However, this value is not an accurate parameter value of R_E. To extract the final R_E we need to use DC Output curves with self-heating and high injection effects. But this optimization could still give us a good estimation and help to set a better range during R_E optimization later compared with default data.

3.5.2 R_{Cc} active

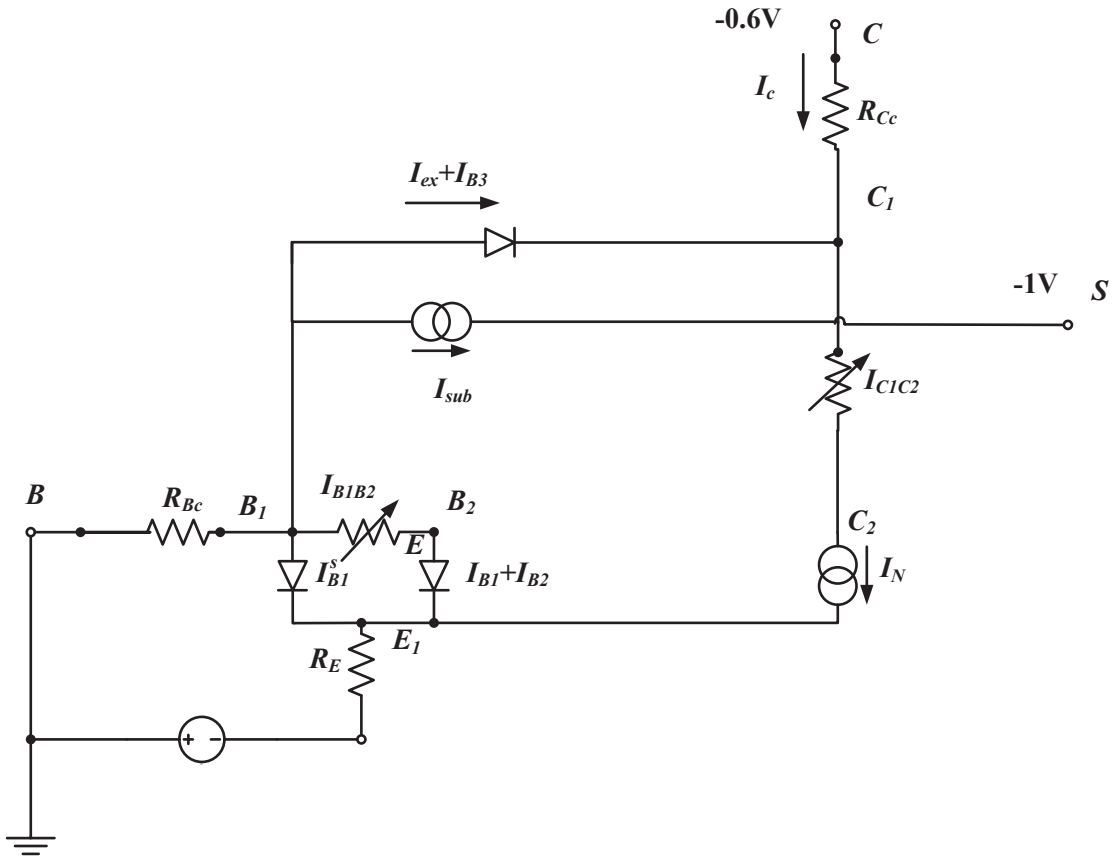

Figure 3.19: R_{Cc}-active measurement simplified circuit [5].

The collector series resistance R_{Cc} can be extracted from the substrate current in the dedicated $R_{Cc} - active$ measurement. The intrinsic base-collector bias can be shown as:

$$V_{B_1C_1} = V_{BC} + R_{Cc}I_C - R_{Bc}I_B, \tag{3.26}$$

We will neglect the voltage drop so the substrate current can be described as:

$$I_{sub} = \frac{2I_{Ss}e^{V_{B_1C_1}/V_T}}{1 + \sqrt{1 + \frac{I_S}{I_{ks}}e^{V_{B1C1}/V_T}}}, \tag{3.27}$$

Substrate current fitting consists of many parts. The value of R_{Cc}, R_{Bc}, and IKS would be important. Since R_{Bc} will be used for optimizing in DC Output curves so here we only focus on R_{Cc} and IKS. R_{Cc} will affect the range between 0.8v to 1.2v and IKS will decide the knee point. At high bias, because of the voltage drop over R_{bcli},$V_{B_1C_4}$ will be smaller than $V_{B_1C_1}$, so the measurement substrate current is smaller than simulated one at high bias. The optimization result is shown in Figure 3.20

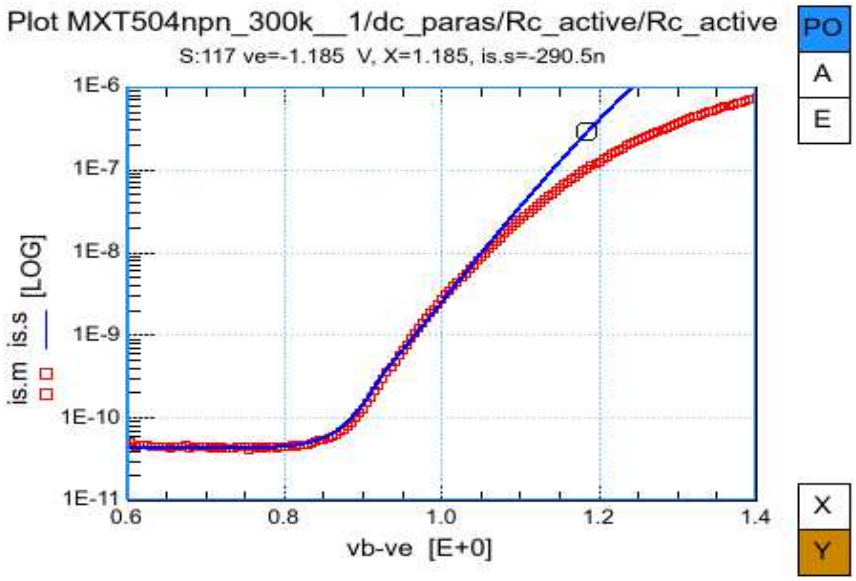

Figure 3.20: Measured(markers) and simulation(line) substrate current

Again with this optimization we could get better initial values of R_{Cc} and R_{Bc}. However, the final value should be decided during DC output curve optimization and iteration back to DC Gummel plots.

3.6 Low Bias DC Output Curves

With low forced base current and low forced V_{BE} environment there are not too much self-heating and high injection effect happening. So under these two setups we can take a look at dc output curves first to verify whether our former parameter extractions are correct and reasonable or not. If we have good values of the extracted parameter we could have good fitting result of dc output curve(I_C versus V_{CE} at constant I_B without any extra optimization. The result is shown below from Figure 3.21 to Figure 3.24.

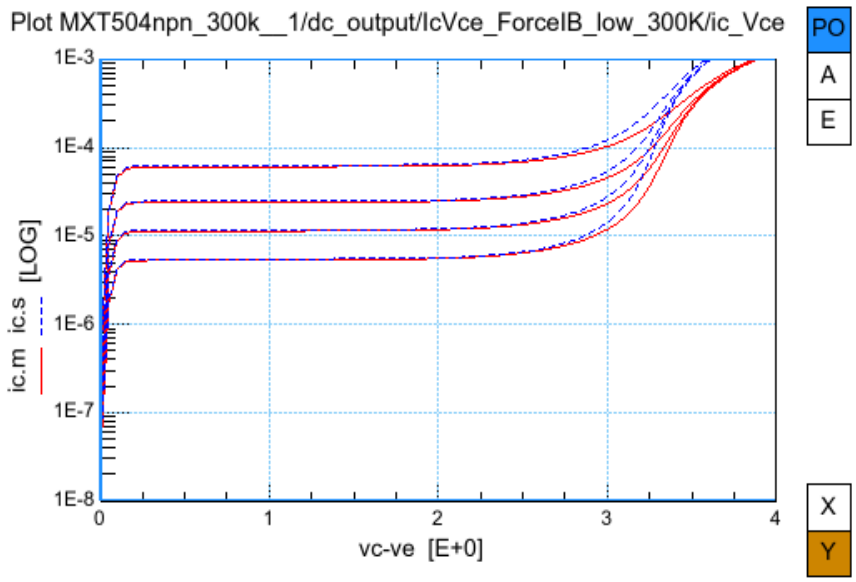

Figure 3.21: Measured(markers) and simulated(line) forced low I_B I_C-V_{CE} plot

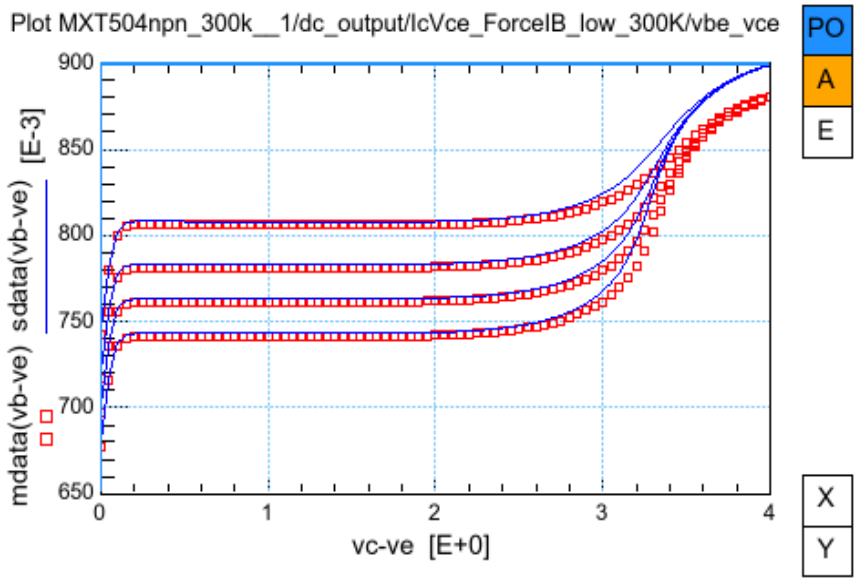

Figure 3.22: Measured(markers) and simulated(line) forced low I_B V_{BE}-V_{CE} plot

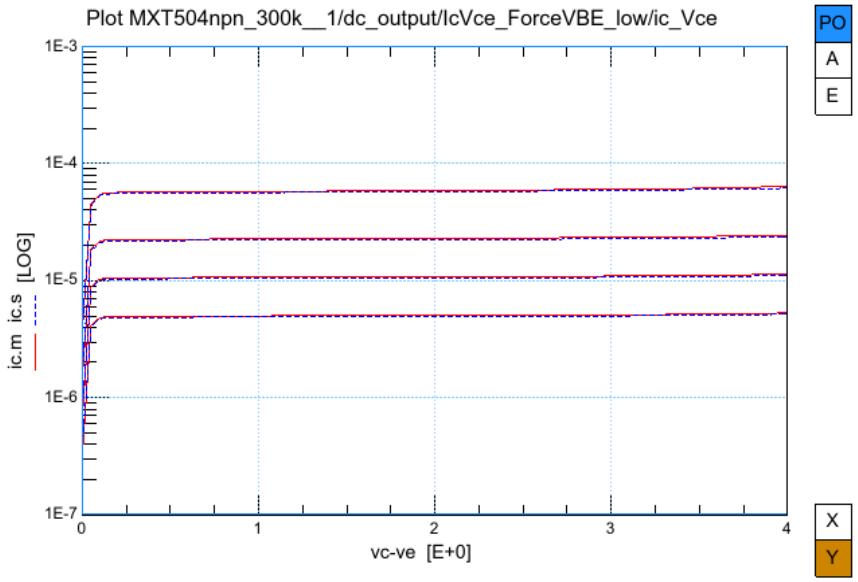

Figure 3.23: Measured(markers) and simulated(line) forced low V_{BE} I_C-V_{CE} plot

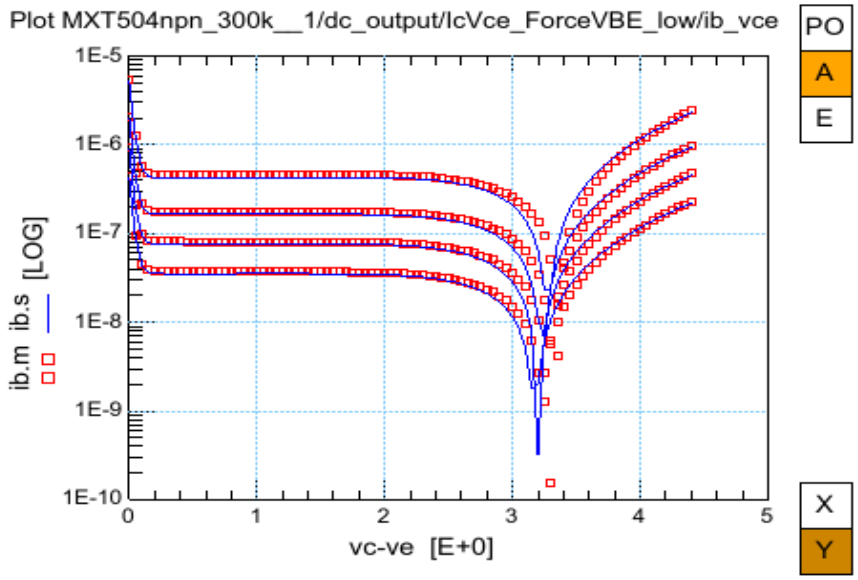

Figure 3.24: Measured(markers) and simulated(line) forced low V_{BE} I_B-V_{CE} plot

3.7 High Bias DC Output Curves

3.7.1 knee current and Ohmic resistance

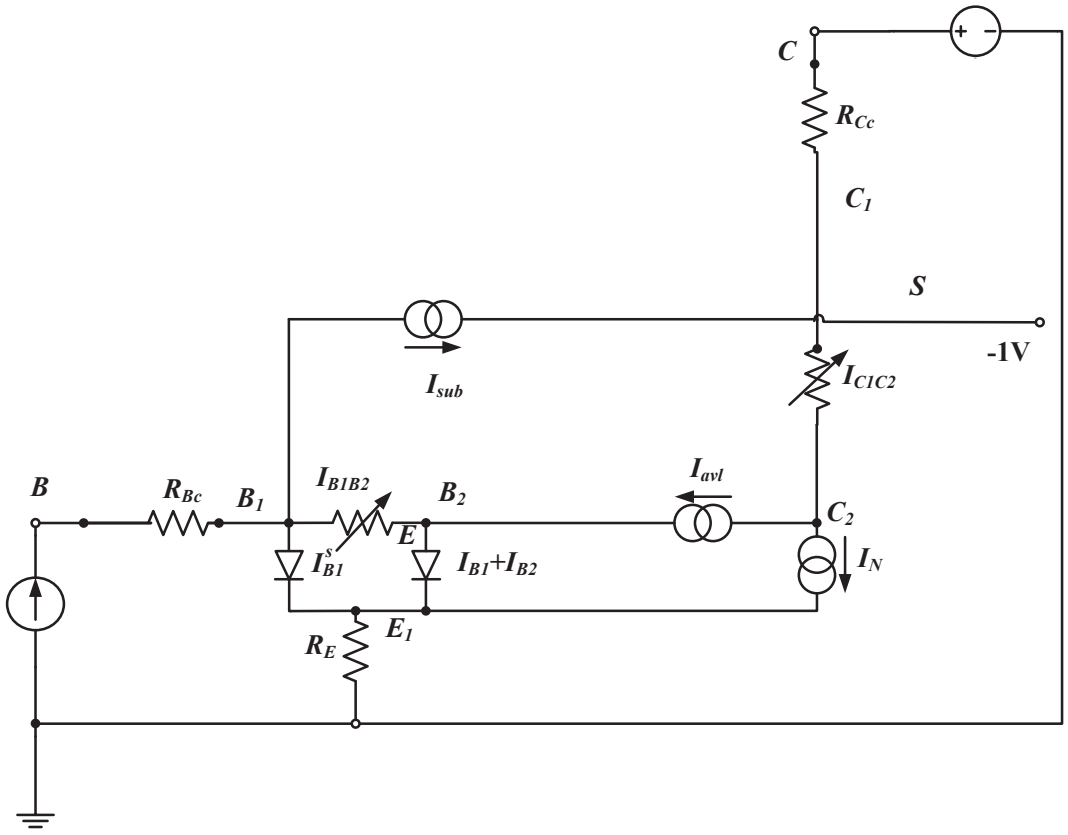

Figure 3.25: Forced I_B output characteristic measurement simplified circuit [5]

At high collector currents and voltages, output curves can present a few physics effects, like quasi saturation, self heating, and high injection effect. Due to self heating effect the device temperature will increase fast which leads to the distortion of the measurement. The collector current at high V_{CE} measurement circuit is shown in Figure 3.25. The collector current is:

$$I_{C_1C_2} = I_{sT} \cdot \frac{e^{V_{B_2E_1}/V_T} - e^{V^*_{B_2C_2}/V_T}}{q_B^I}, \tag{3.28}$$

The collector current increases sharply as the collector-emitter bias increases from 0V. At this hard saturation region we can extract R_{Cc}. Then quasi saturation effect happens when

V_{CE} increases. R_{Cv} can be extracted at this part. As V_{CE} keep increasing collector current curve becomes flat but increases slowly as the saturation current increase with increasing power dissipation. We can extract knee current at this region. Because of the high V_{CE} the self heating effect happens. It increases ΔT and makes the temperature scaling effect significantly. Thus R_{th} and temperature coefficient parameter AB which is related to I_{sT} and I_{kT} can be optimized to help plots fitting. At high collector-emitter bias, the collector current increase because the avalanche effect. In this thesis the avalanche model has bad current dependency at high current range. So even though we have a good G_{em} parameters extraction at low current range earlier, the avalanche effect part in output curves under high bias forced I_B setup may not fit very well. R_{th} also needs to be The strategy is shown in Figure 3.26. In my optimization experience tuning AB can cause big change in I_C-V_{CE} curves. It will also be used in R_{th} extraction and τ_B temperature scaling optimization. So we need to extract AB here and do a iteration optimization when we do R_{th} and cutoff frequency temperature scaling. The sensitivity of AB to I_C is shown from Figure 3.27 to Figure 3.28.

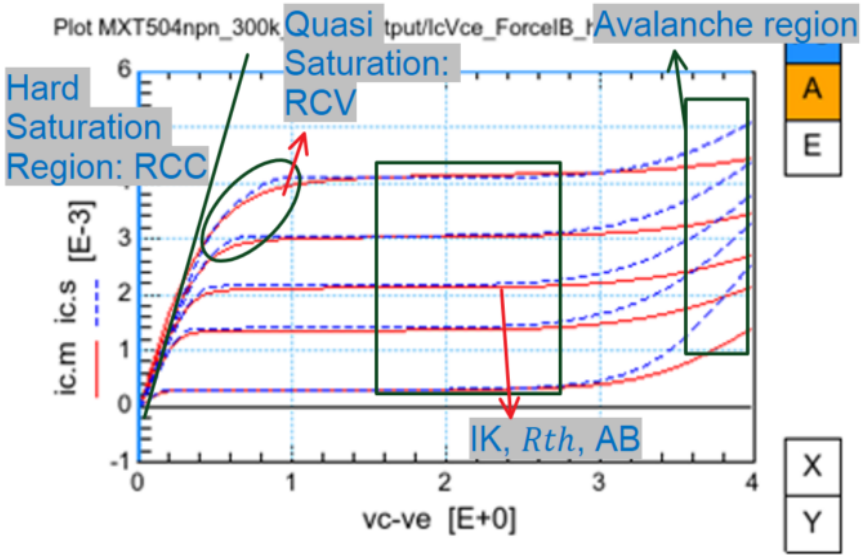

Figure 3.26: Measured(markers) and simulated(line) DC output I_C-V_{CE}

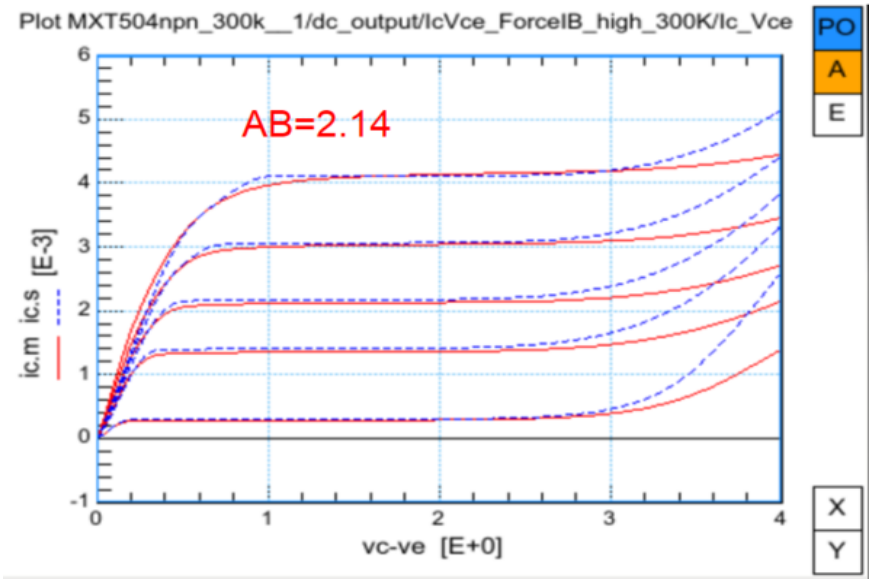

Figure 3.27: Measured(markers) and simulated(line) I_C-V_{CE} when AB is extracted

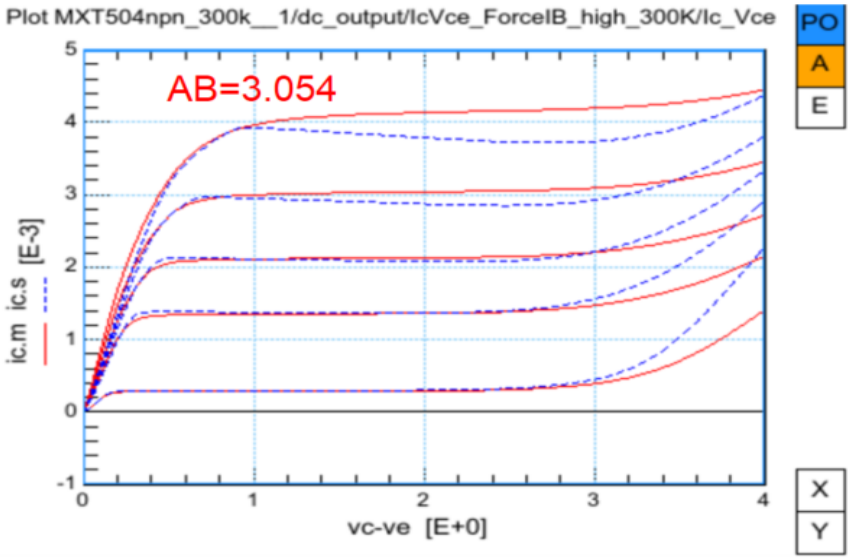

Figure 3.28: Measured(markers) and simulated(line) I_C-V_{CE} when AB increases

3.7.2 Self Heating Parameters Extraction

For the high current parameters we will need to include temperature scaling rules. The equations are shown in Chapter 5. Thermal resistance R_{th} is extracted from the base emitter voltage at high V_{CE} using the output-characteristic measurements shown in Figure 3.25. Since the junction temperature is determined by the thermal resistance for a given power dissipation, accurate modeling of the thermal resistance R_{th} is critical for the modeling of junction temperature. Due to the self-heating the temperature of the transistor rises with an amount of:

$$\Delta T = R_{th} \left(I_B V_{BE} + I_C V_{CE} \right), \tag{3.29}$$

The collector part is the most important to self-heating and the values of R_{th} are about 100-500 °C/W. The temperature will increase with the increase of V_{CE}, and V_{BE} can be express by:

$$V_{BE} \simeq V_T ln \left(\frac{I_B \beta_{fT}}{I_{ST}} \right) + I_C R_{ET}, \tag{3.30}$$

From I_C-V_{CE} plot we can see that when V_{CE} is between 1V and 2.5V I_C is flat. According to the initialization A_E is zero. So based on the equation at fixed I_B the drop of V_{BE} is dominated by I_S and β_f temperature scaling. At flat I_C and fixed I_B the temperature scaling of β_f is related to I_{KT}. Because I_K temperature scaling is decided by A_B, and I_{ST} is also A_B related. Because A_E is set to zero, R_E doesn't have temperature scaling during simulation. So we can extract R_E at left corner of V_{BE}-V_{CE} plot when self heating hasn't happen yet. Then we can open I_C-V_{CE} plot and use plot optimizer to fit both plots. Then we can get R_{th} and A_B values. However, when we do the optimization of temperature scaling, it will need R_{th} and A_B again. So the final value will be extracted later. The optimization result is shown from Figure 3.30 to Figure 3.33.

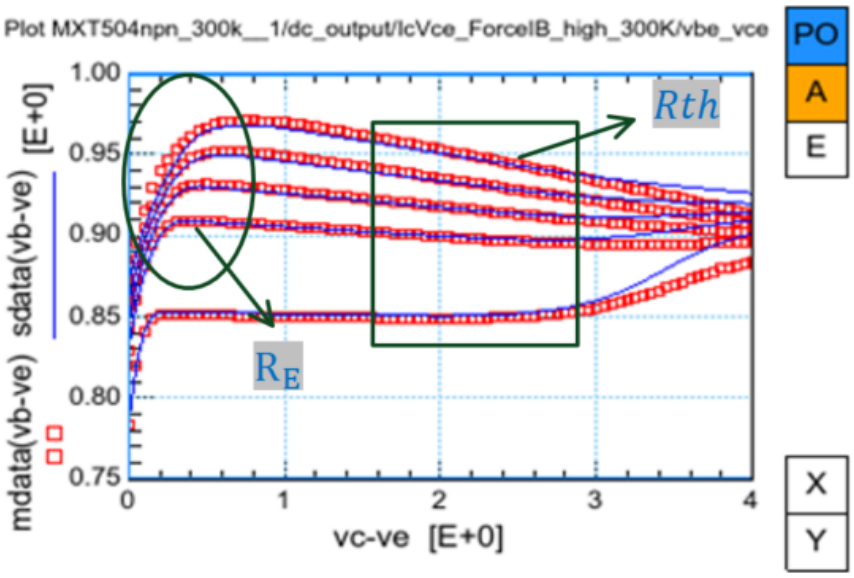

Figure 3.29: Measured(markers) and simulation(line) DC output V_{BE}-V_{CE}

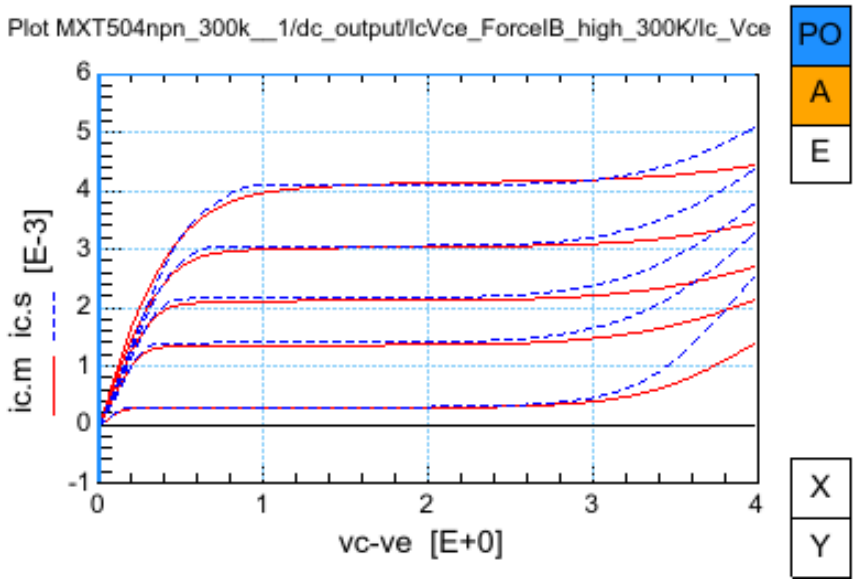

Figure 3.30: Measured(markers) and simulated(line) forced I_B high I_C-V_{CE} plot

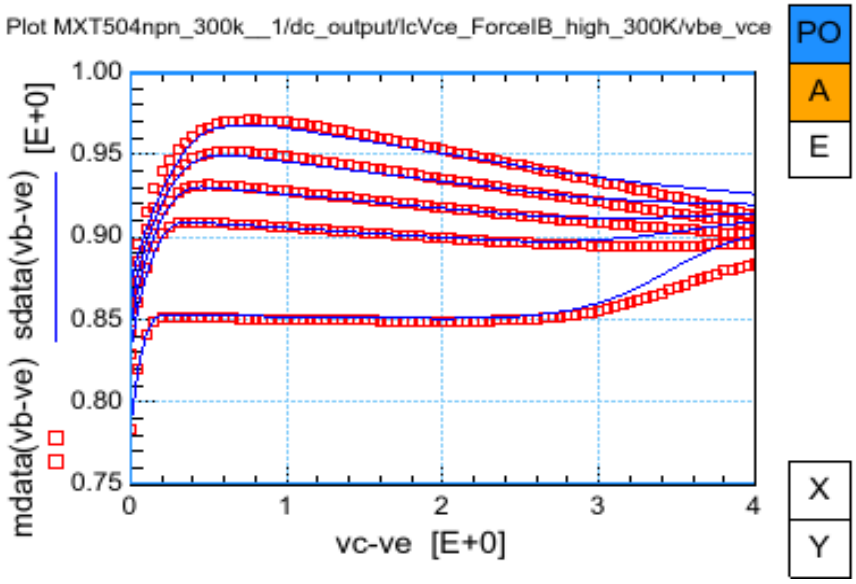

Figure 3.31: Measured(markers) and simulated(line) forced I_B high V_{BE}-V_{CE} plot

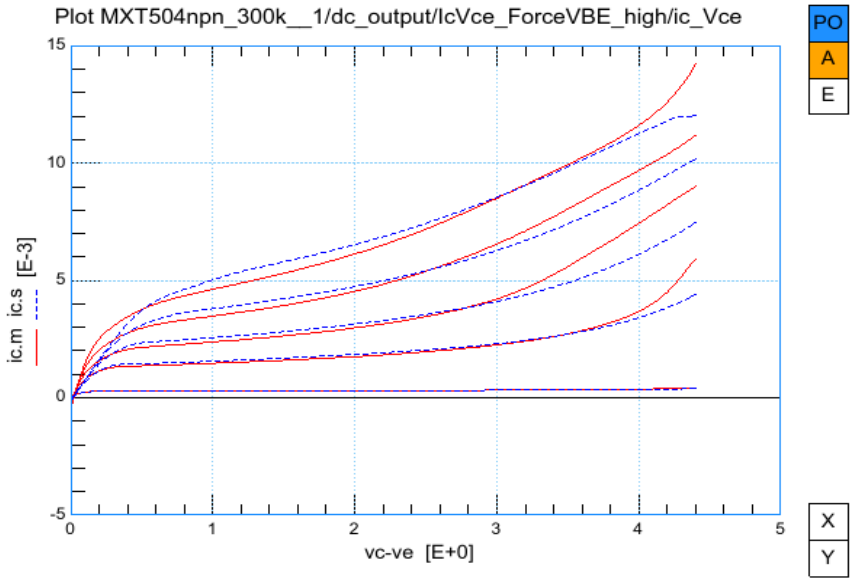

Figure 3.32: Measured(markers) and simulated(line) forced V_{BE} high I_C-V_{CE} plot

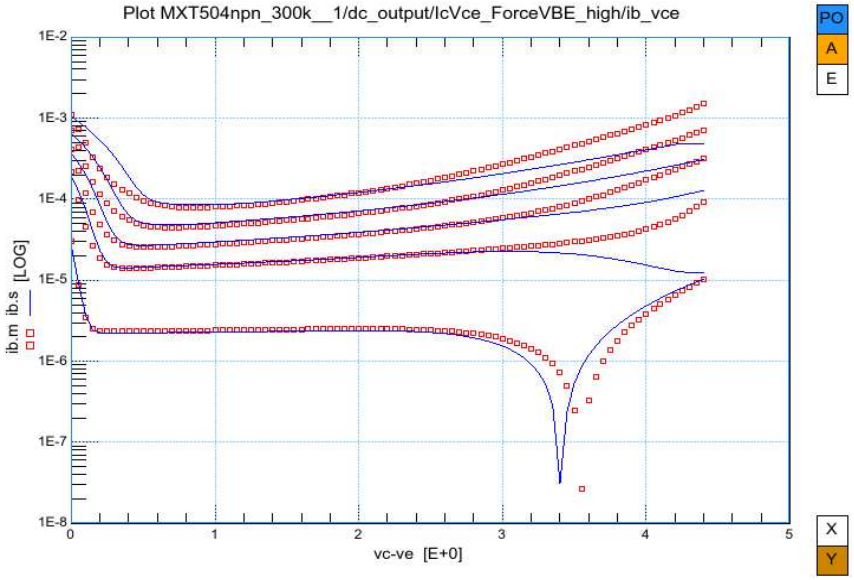

Figure 3.33: Measured(markers) and simulated(line) forced V_{BE} high I_B-V_{CE} plot

3.8 DC Plots Check

After dc output curves fitting, we can take a look back at all dc curves with new extracted parameters. With most of the high injection effect and self heating parameters extraction included in DC output curve fitting, the DC curves after simulations should be ideal now. A few parameters may need to be optimized to fit all important curves. The final dc parameter extraction strategy is shown in Table 3.1.

Base-emitter cap.	C_{jE}, p_E, V_{dE}
Base-collector cap.	C_{jC}, p_C, X_p
Substrate-collector cap.	C_{jS}, p_S, V_{dS}
Avalanche	W_{avl}, V_{avl}
Early Effect	V_{ER}, V_{EF}, DEG
Forward-Gummel I_C	I_s
Forward-Gummel I_B	β_f, I_{Bf}, m_{Lf}
Reverse-Gummel I_{sub}	I_{Ss}
Reverse-Gummel hfc	β_{ri}, I_{Br}, V_{Lr}
DC Paras I_{sub}	I_{ks}
Output Forced V_{BE} high	R_{th}, R_E
Output Forced I_B high	I_K, R_{Cc},R_{Cv}
Forward-Gummel hfe	V_{dC},
Reverse-Gummel hfc	R_{Bc}

Table 3.1: DC Parameters Extraction Strategy Final Check

There are still a few DC parameters, like R_{Bv}, I_{CSS},R_{Cblx}, R_{Cbli}, are not extracted yet. R_{Bv} and R_{Cv} can be extracted in Y-parameters fitting and cutoff frequency fitting. But in this thesis R_{Cblx} and R_{Bli} are not considered. Without Zener tunneling current considered, *NZEB* and *IZEB* are not extracted. With *EXAVL*=0, *SFH* is not extracted. A few factor parameters like *XCJC*, *XCJE* are not extracted as well.

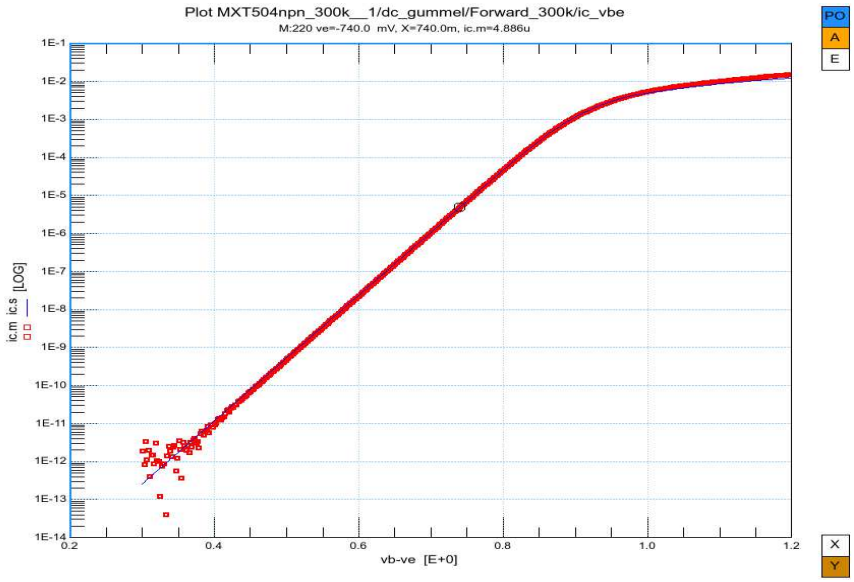

Figure 3.34: Measured(markers) and simulated(line) I_C in forward Gummel Measurement.

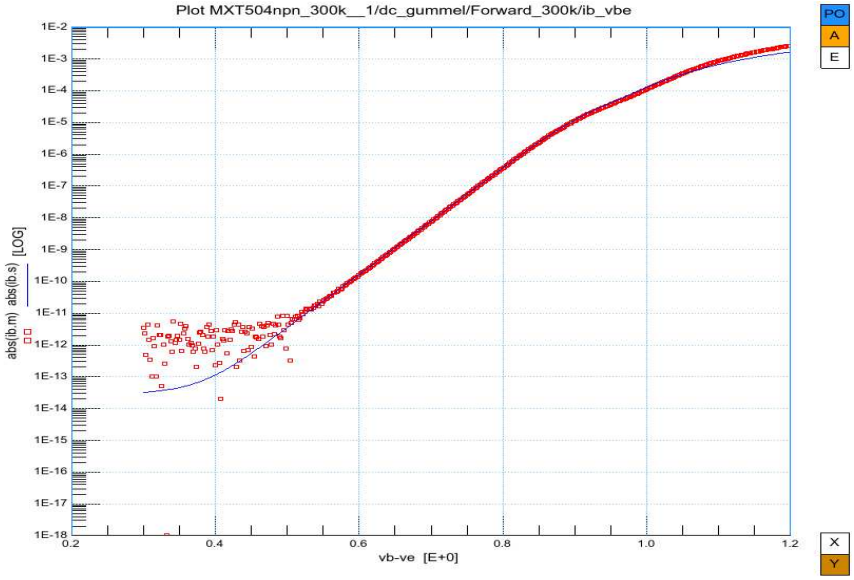

Figure 3.35: Measured(markers) and simulated(line) I_B in forward Gummel Measurement.

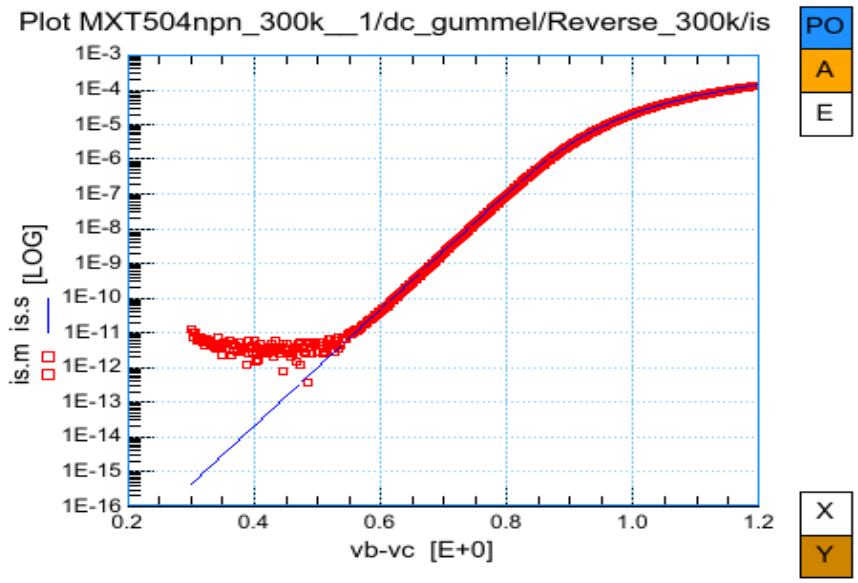

Figure 3.36: Measured(markers) and simulated(line) I_{sub} in reverse Gummel Measurement.

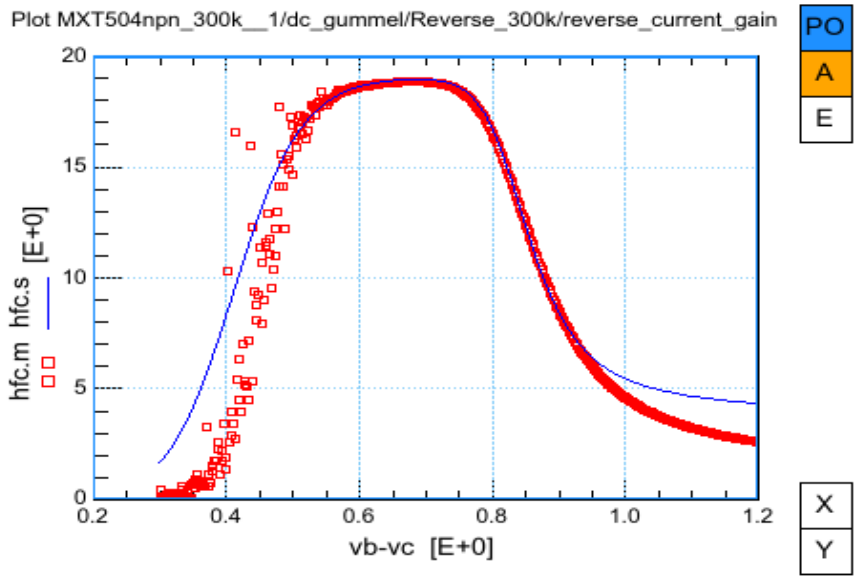

Figure 3.37: Measured(markers) and simulated(line) reverse current gain in reverse Gummel Measurement.

3.9 Parameter Extraction Conflicts

As shown is Figure 3.38, after dc parameter extraction is done, the DC Parameter substrate current shows a very bad fitting result. However, most of other dc characteristic plots fitting are great. It shows some part of the dc parameters have errors but the overall is great. Try to keep most of important plots good, we have to make a compromise to sacrifice this plot.

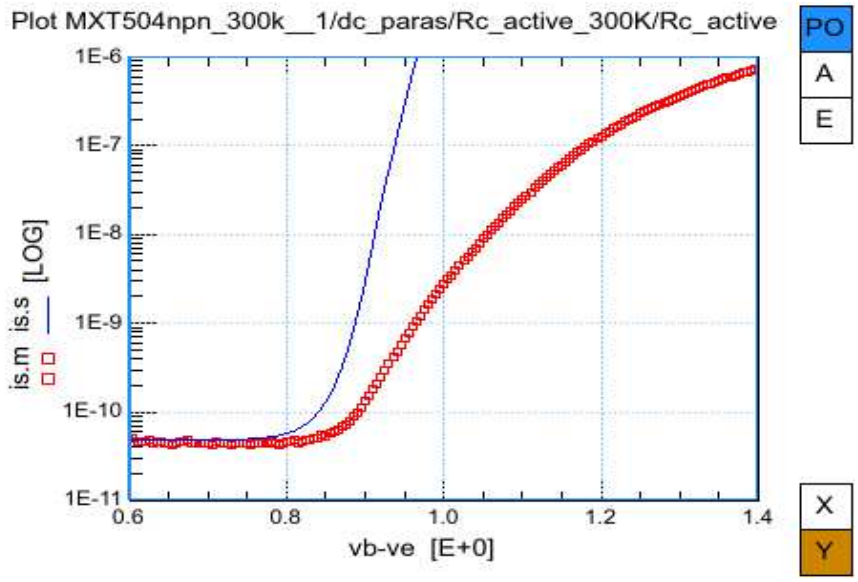

Figure 3.38: Measured(markers) and simulated(line) DC Parameter substrate current after DC Output fitting

Chapter 4

Extraction of AC Parameters

4.1 cutoff frequency

In Mextram model curoff frequency is defined as the frequency where the current gain h_{fe} becomes unity. [8]

$$f_T = \frac{f}{Im(\frac{1}{h_{fe}})} \tag{4.1}$$

At AC parameter extraction, based on simulation we need to calculate f_T through Y-parameters:

$$h_{fe} = h_{21} = \frac{Y_{21}}{Y_{11}} \tag{4.2}$$

Since all the measurement data we have are S-parameters so we need a program here to calculate f_T :

```
Sdut_raw:
spar=Meas
return spar


Ydut:
Ydut_raw=TwoPort(Sdut_raw,"S","Y")
Yd=Ydut_raw
print"end Ydut"
return Yd


fT:
return freq*abs(Ydut.21//Ydut.11)
```

From f_T curves we can extract $SCRCV$, I_{hc}, AXI, and the transit times parameters. I_{hc}, $SCRCV$, τ_B, τ_E, and m_τ should be extracted around peak of cutoff frequency. Based

on verilogA code of Mextram, τ_E and m_τ should be optimized together at all time. At the region of post peak cutoff frequency we can extract τ_{epi} and AXI. Extraction strategy is shown in Figure 4.1. The cutoff frequency verse I_C curves at different V_{CB} results are shown from Figure 4.2 to Figure 4.5.

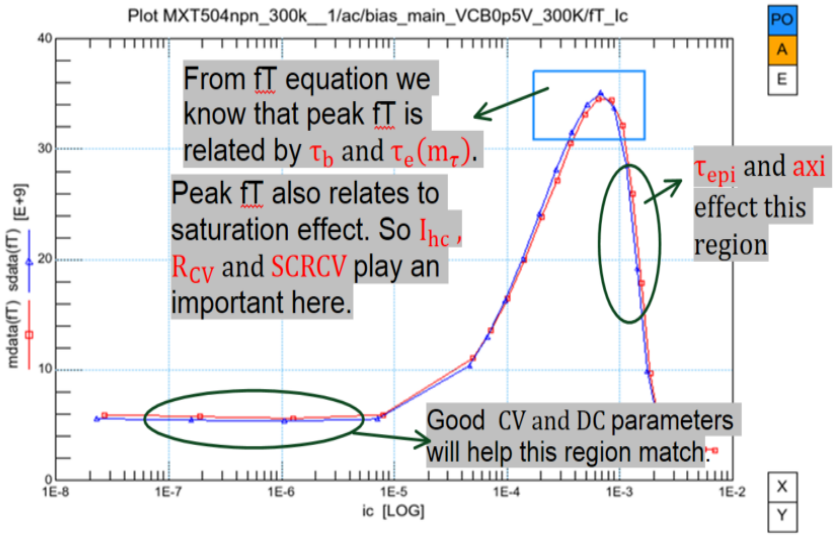

Figure 4.1: Cutoff frequency optimization strategy.

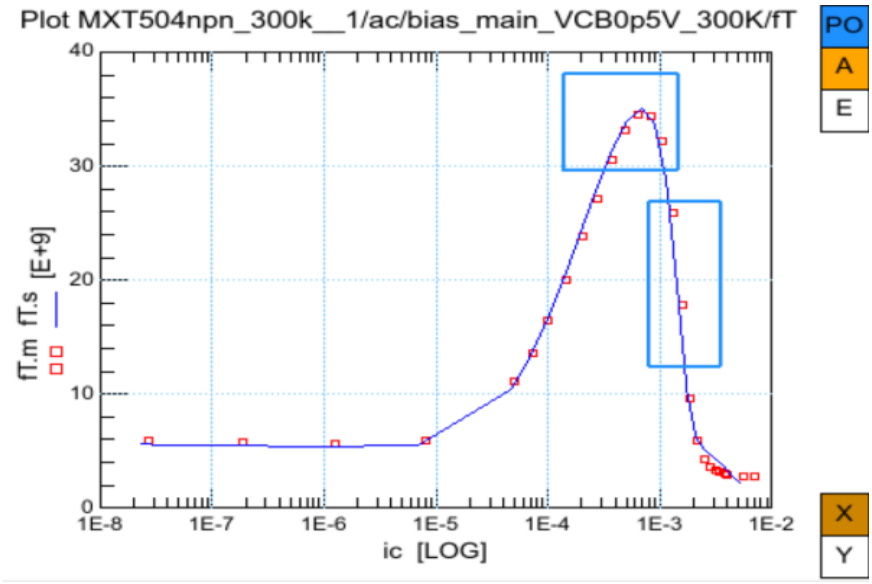

Figure 4.2: Measured(markers) and calculated(line) cut-off frequency at V_{CB}=-0.5V

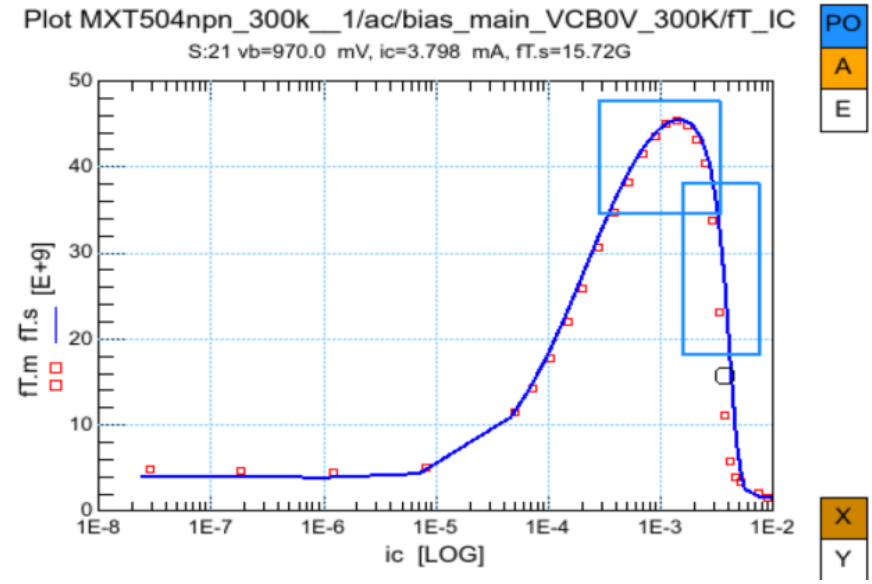

Figure 4.3: Measured(markers) and calculated(line) cut-off frequency at V_{CB}=0V

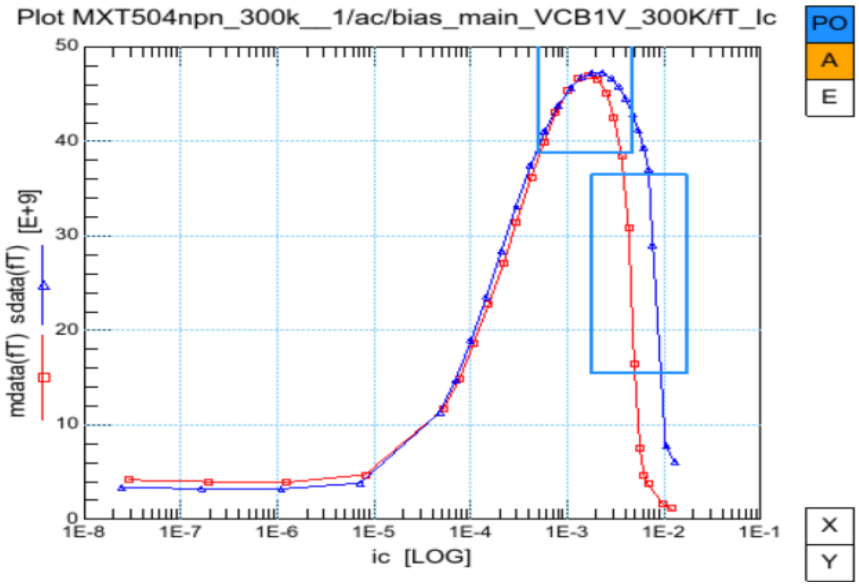

Figure 4.4: Measured(markers) and calculated(line) cut-off frequency at V_{CB}=1V

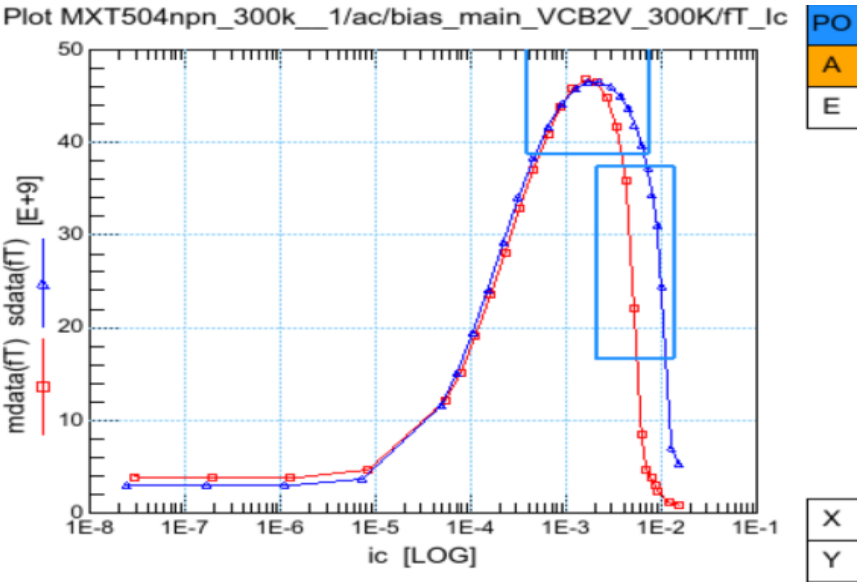

Figure 4.5: Measured(markers) and calculated(line) cut-off frequency at V_{CB}=2V

Chapter 5

Temperature Scaling

5.1 Temperature scaling rules

The parameters we have already extracted is at room temperature(300K). But in real life the component should fit different temperatures. In this case we need to put temperature scaling into account. In Table 5.1 the cross reference between the temperature parameters and the electrical parameters is listed [4].

The actual simulation temperature is denoted by TEMP (in °C). The temperature at which the parameters are determined is $\mathrm{T_{ref}}$ (also in °C).

Conversion to Kelvin

$$T_K = \mathrm{TEMP} + \mathrm{DTA} + 273.15 + \mathrm{V_{dT}}, \tag{5.1a}$$

$$T_{\mathrm{amb}} = \mathrm{TEMP} + \mathrm{DTA} + 273.15, \tag{5.1b}$$

$$T_{RK} = \mathrm{T_{ref}} + 273.15, \tag{5.2}$$

$$t_N = \frac{T_K}{T_{RK}}, \tag{5.3}$$

Depletion capacitance The junction diffusion voltages $\mathrm{V_{d_E}}$, $\mathrm{V_{d_C}}$, and $\mathrm{V_{d_S}}$ with respect to temperature are

$$U_{d_E T} = -3\, V_T\ \ln t_N + \mathrm{V_{d_E}}\ \mathrm{t_N} + (1 - \mathrm{t_N})\ \mathrm{V_{g_B}}, \tag{5.4}$$

1	A_{QB0}	V_{er}, V_{ef}, I_s, β_f, R_{Bv}, τ_B, τ_R, I_{ks}, dE_g
2	A_E	R_E, β_f
3	A_B	R_{Bv},β_f,I_s,I_k τ_B, τ_R, τ_E, I_{ks}
4	A_{epi}	R_{c_v}, τ_{epi}, τ_R
5	A_{ex}	R_{B_C}
6	A_C	R_{C_C}
7	A_S	I_{S_S}, I_{ks}
8	$dV_{g\beta r}$	β_{ri}
9	V_{g_B}	I_s, C_{j_E}, V_{d_E}, V_{er}, I_{ks}
10	V_{g_C}	C_{j_C}, V_{d_C}, X_p, I_{Br}, V_{ef}
11	V_{g_j}	I_{Br}
12	$dV_{g\tau_E}$	τ_E
13	V_{g_S}	I_{S_S}, I_{ks}, C_{j_S}, V_{d_S}
14	$dV_{g\beta f}$	β_f

Table 5.1: Summary of the occurrence of the temperature parameters in the temperature scaling rules of the electrical parameters[8].

$$\mathrm{V_{d_ET}} = \mathrm{U}_{d_E T} + \mathrm{V_T} \ln\{1 + \exp[(\mathrm{V_{d,low}} - \mathrm{U}_{d_E T})/\mathrm{V_T}]\}, \tag{5.5}$$

$$U_{d_C T} = -3\, V_T\ \ln t_N + \mathrm{V_{d_C}}\ \mathrm{t_N} + (1 - \mathrm{t_N})\ \mathrm{V_{g_C}}, \tag{5.6}$$

$$\mathrm{V_{d_CT}} = \mathrm{U}_{d_C T} + \mathrm{V_T} \ln\{1 + \exp[(\mathrm{V_{d,low}} - \mathrm{U}_{d_C T})/\mathrm{V_T}]\}, \tag{5.7}$$

$$U_{d_S T} = -3\, V_T\ \ln t_N + \mathrm{V_{d_S}}\ \mathrm{t_N} + (1 - \mathrm{t_N})\ \mathrm{V_{g_S}}, \tag{5.8}$$

$$\mathrm{V_{d_ST}} = \mathrm{U}_{d_S T} + \mathrm{V_T} \ln\{1 + \exp[(\mathrm{V_{d,low}} - \mathrm{U}_{d_S T})/\mathrm{V_T}]\}. \tag{5.9}$$

The zero-bias capacitance scale with temperature as

$$\mathrm{C_{j_ET}} = \mathrm{C_{j_E}}\ \left(\frac{\mathrm{V_{d_E}}}{\mathrm{V_{d_ET}}}\right)^{\mathrm{p_E}}, \tag{5.10}$$

$$C_{jsT} = C_{js} \left(\frac{V_{dS}}{V_{dsT}} \right)^{pS}, \tag{5.11}$$

The collector depletion capacitance is divided in a variable and a constant part. The constant part is temperature independent.

$$C_{jcT} = C_{jc} \left[(1 - X_p) \left(\frac{V_{dC}}{V_{dcT}} \right)^{pC} + X_p \right], \tag{5.12}$$

$$X_{pT} = X_p \left[(1 - X_p) \left(\frac{V_{dC}}{V_{dcT}} \right)^{pC} + X_p \right]^{-1}. \tag{5.13}$$

Resistances The various parameters A describe the mobility of the corresponding regions: $\mu \propto t_N^{-A}$. The temperature dependence of the zero-bias base charge goes as $Q_{B0T}/Q_{B0} = t_N^{A_{QB0}}$.

$$R_{ET} = R_E \, t_N^{A_E}, \tag{5.14}$$

$$R_{BvT} = R_{Bv} \, t_N^{A_B - A_{QB0}}, \tag{5.15}$$

$$R_{BcT} = R_{Bc} \, t_N^{A_{ex}}, \tag{5.16}$$

$$R_{CvT} = R_{Cv} \, t_N^{A_{epi}}, \tag{5.17}$$

$$R_{CcT} = R_{Cc} \, t_N^{A_C}. \tag{5.18}$$

Current gains

$$\beta_{fT} = \beta_f \, t_N^{A_E - A_B - A_{QB0}} \, \exp[-dV_{g\beta f}/V_{\Delta T}], \tag{5.19}$$

$$\beta_{riT} = \beta_{ri} \, \exp[-dV_{g\beta r}/V_{\Delta T}], \tag{5.20}$$

Currents and voltages

$$I_{sT} = I_s \, t_N^{4 - A_B - A_{QB0} + dA_{Is}} \, \exp[-V_{gB}/V_{\Delta T}], \tag{5.21}$$

$$I_{kT} = I_k \; t_N^{1-A_B}, \tag{5.22}$$

$$I_{BfT} = I_{Bf} \; t_N^{(6-2m_{Lf})} \; \exp[-V_{g_j}/m_{Lf} \; V_{\Delta T}], \tag{5.23}$$

$$I_{BrT} = I_{Br} \; t_N^2 \; \exp[-V_{g_C}/2V_{\Delta T}], \tag{5.24}$$

$$V_{efT} = V_{ef} \; t_N^{A_{Q_{B0}}} \; \left[(1 - X_p) \; \left(\frac{V_{d_C}}{V_{d_C T}}\right)^{p_C} + X_p\right]^{-1}, \tag{5.25}$$

$$V_{erT} = V_{er} \; t_N^{A_{Q_{B0}}} \; \left(\frac{V_{d_E}}{V_{d_E T}}\right)^{-p_E}, \tag{5.26}$$

The temperature dependence of I_{Ss} andI_{ks} is given by A_S and V_{g_S}.

A_S equals A_C for a closed buried layer (BN) and A_S equals A_{epi} for an open buried layer.

$$I_{SsT} = I_{Ss} \; t_N^{4-A_S} \; \exp[-V_{g_S}/V_{\Delta T}], \tag{5.27}$$

$$I_{ksT} = I_{ks} \; t_N^{1-A_S} \; \frac{I_{sT}}{I_s} \; \frac{I_{Ss}}{I_{SsT}}, \tag{5.28}$$

When either $I_s = 0$ or $I_{SsT} = 0$ we take $I_{ksT} = I_{ks} \; t_N^{1-A_S}$.

Transit times

$$\tau_{ET} = \tau_E \; t_N^{(A_B-2)} \; \exp[-dV_{g_{\tau_E}}/V_{\Delta T}], \tag{5.29}$$

$$\tau_{BT} = \tau_B \; t_N^{A_{Q_{B0}}+A_B-1} \tag{5.30}$$

$$\tau_{epiT} = \tau_{epi} \; t_N^{A_{epi}-1}, \tag{5.31}$$

$$\tau_{RT} = \tau_R \; \frac{\tau_{BT} + \tau_{epiT}}{\tau_B + \tau_{epi}}. \tag{5.32}$$

5.2 Temperature parameters extraction

5.2.1 CV temperature scaling

Capacitance temperature scaling equations are shown as below:

$$C_{beT} = C_{jET} * (\frac{V_{dET}}{V_{dE}})^{p_E}, \tag{5.33}$$

$$C_{bcT} = C_{jCT} * ((1 - X_p) * (\frac{V_{dCT}}{V_{dC}})^{p_C} + X_p), \tag{5.34}$$

$$C_{scT} = C_{jST} * (\frac{V_{dST}}{V_{dS}})^{p_S}, \tag{5.35}$$

From C_{beT} equation we can see that the temperature scaling of C_{be} is related to C_{jE}, V_{dE} and p_E. C_{jE}'s and V_{dE}'s temperature scaling is decided by V_{gB}. Then open optimizer we can get a plot like Figure 5.1.

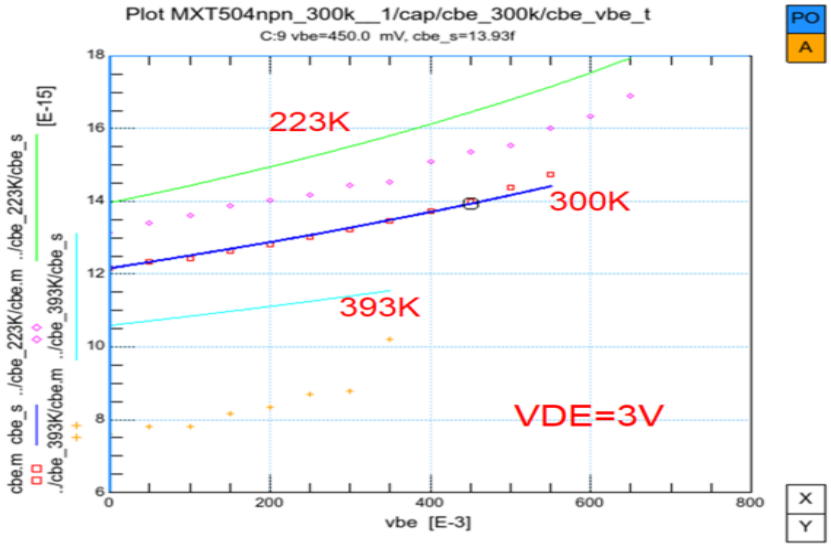

Figure 5.1: Measured(markers) and simulated(line) collector base capacitance temperature scaling with V_{DE}=3V.

However, V_{dE}=3V is unacceptable. V_{dE} is an important parameter which is widely used in Gummel curves and other dc characteristics. A large V_{dE} will mess up all other plots. So in a reasonable range the Temperature scaling of Cbe is shown in Figure 5.2.

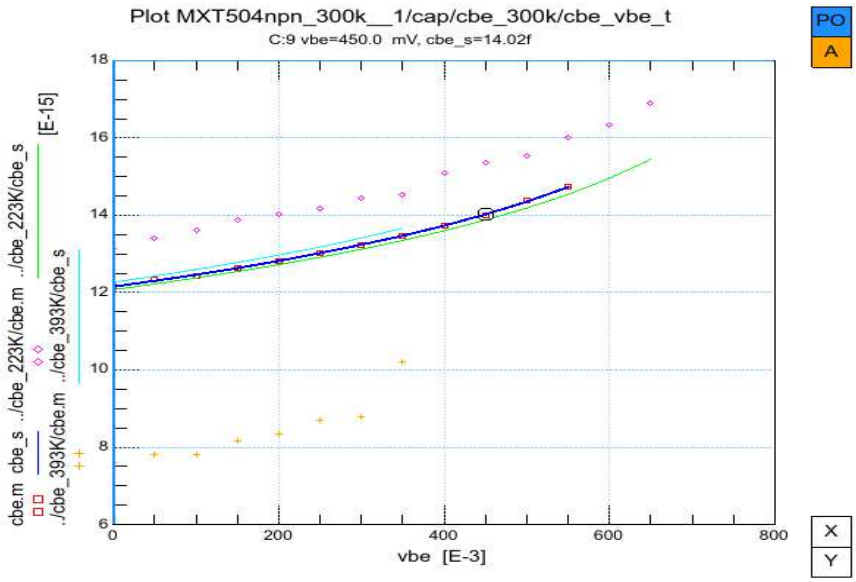

Figure 5.2: Measured(markers) and simulated(line) collector base capacitance scaling

The same problem happens at C_{sc} as well. The temperature scaling of C_{sc} is shown in Figure 5.3.In the future we need more data to find out the real capacitance temperature scaling.

However, the temperature scaling of C_{bc} shows well. You can see the temperature scale well from 223K to 393K in Figure 5.4.

5.2.2 AQB0

From Table 5.1 we can see that A_{QB0} is one of the most important temperature coefficient parameters. It is used in many parameter's temperature scaling equations. So extract a good value of A_{QB0} is essential. It can help to improve the accuracy of later temperature coefficient parameter extraction.

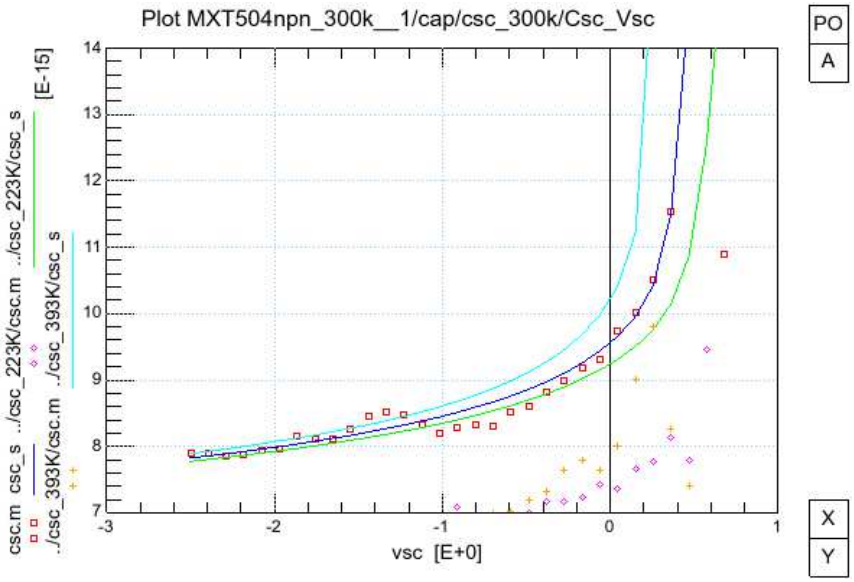

Figure 5.3: Measured(markers) and simulated(line) collector substrate capacitance temperature scaling

According to the table, V_{er}, V_{ef}, and dE_g only use A_{QB0} for temperature scaling. So we choose these three parameters for extracting A_{QB0}.

$$V_{efT} = V_{ef} \cdot exp(lntN \cdot A_{QB0}) \cdot \frac{1}{X_p + (1 - X_p) \cdot pow(V_{DC}/V_{DC}T, PC)}, \tag{5.36}$$

$$DEG_T = DEG \cdot exp(lntN \cdot A_{QB0}), \tag{5.37}$$

$$V_{erT} = V_{er} \cdot exp(lntN \cdot A_{QB0}) \cdot \frac{1}{pow(V_{DE} \cdot invV_{DE}T, p_E)}, \tag{5.38}$$

Since we have good V_{DC} temperature scaling, we could focus on V_{efT} and DEG_T to extract A_{QB0}. The fitting result is shown in Figure 5.5 to Figure 5.6.

5.2.3 VGB

$$I_{ST} = I_S \cdot exp(lntN \cdot (4 - A_B - A_{QB0} + DAIS)) \cdot exp[-V_{gB} \cdot (\frac{1}{vT} - \frac{1}{vTr}], \tag{5.39}$$

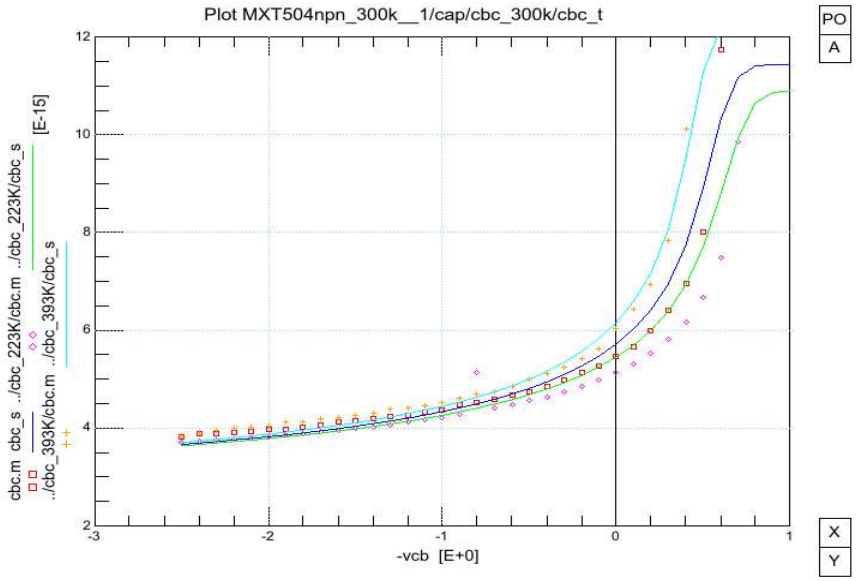

Figure 5.4: Measured(markers) and simulated(line) collector base capacitance temperature scaling

From this equation we can see that IS's temperature scaling is decided by AB, A_{QB0}, $DAIS$, and V_{gB}. Since we have extracted a good value of AB and A_{QB0}, $DAIS$ is zero, here we just need to optimize V_{gB}. The fitting result is shown in Figure 5.7.

5.2.4 DVGBF, VGJ, and AEX

$$\beta_{fT} = \beta_f \cdot exp(lntN(A_E - A_B - A_{QB0})) \cdot exp[-DVGBF \cdot (\frac{1}{vT} - \frac{1}{vTr}], \tag{5.40}$$

$$I_{BFT} = I_{BF} \cdot exp(lntN \cdot (6 - 2 \cdot MLF)) \cdot exp(-V_{gJ} \cdot \frac{V_{dtINV}}{MLF}), \tag{5.41}$$

$$R_{BCT} = R_{BC} \cdot exp(lntN \cdot A_{ex}), \tag{5.42}$$

Through these two equations, we can see that the temperature scaling rules of β_f and I_{BF} are related to temperature parameters A_E, A_B, A_{QB0}, $DVGBF$, and V_{gJ}. From former

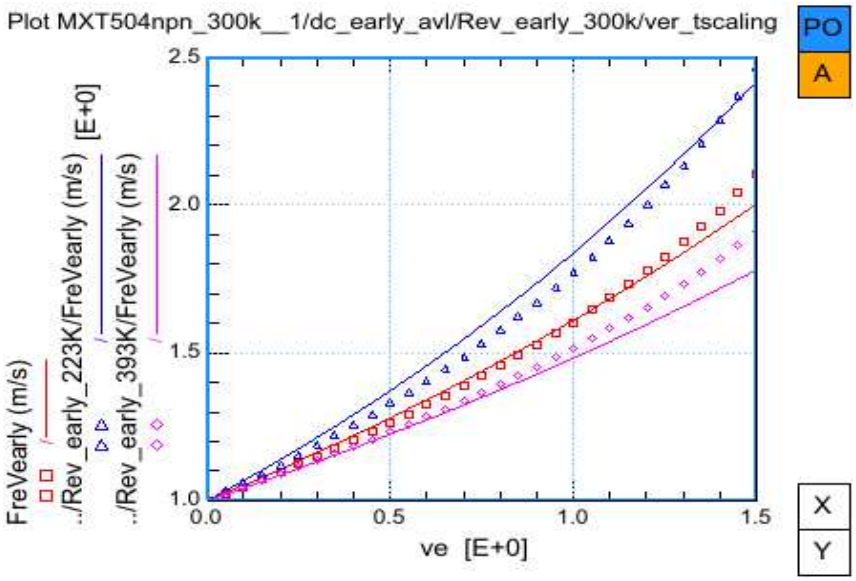

Figure 5.5: Measured(markers) and simulated(line) Ver temperature scaling

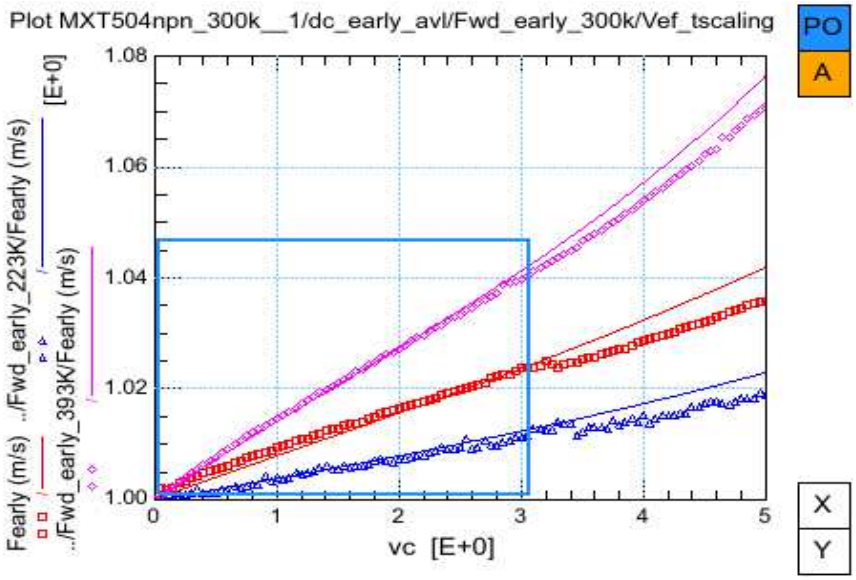

Figure 5.6: Measured(markers) and simulated(line) Vef temperature scaling

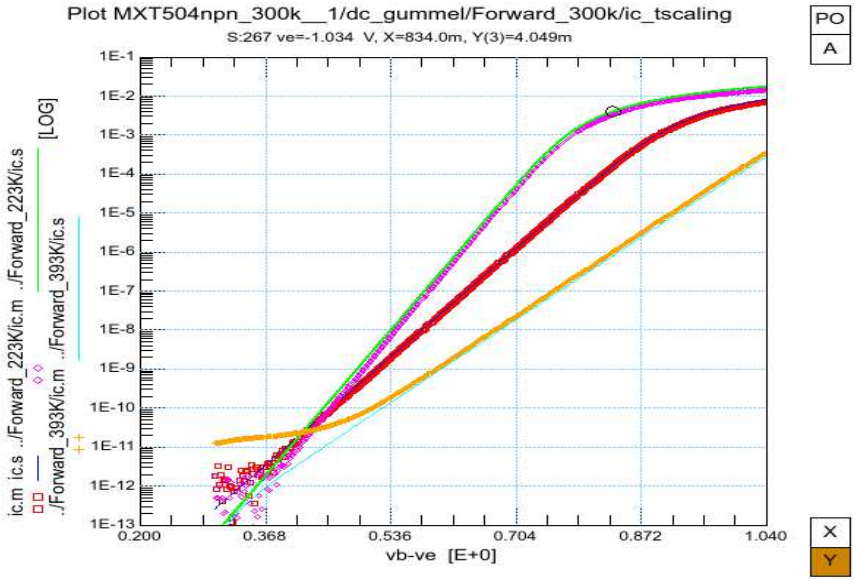

Figure 5.7: Measured(markers) and simulated(line) collector current temperature scaling

extraction we have found A_B and A_{QB0}. A_E is zero here. Even though A_E is also used here but here it doesn't provide any temperature scaling. So we need to find $DVGBF$ and V_{gJ}. We already know that β_f and I_{BF} can influence I_B. By fitting temperature scaling of I_B plots, we can extract $DVGBF$ and V_{gJ}. At I_B curve the high injection part is mainly effected by R_{Bc}. The temperature scaling of R_{Bc} is decided directly by A_{ex}. So by optimizing A_{ex} we can fit the high injection part of I_B in different temperatures. The final fitting plot is shown in Figure 5.8.

5.2.5 VGS and AS

We extracted I_{Ss} by fitting substrate current in low injection range during 300K parameter extraction. So by fitting substrate currents in different temperatures, we need to find out the temperature scaling characteristic of I_{Ss}. Base on the equation,

$$I_{SsT} = I_{Ss} \cdot exp(lntN \cdot (4 - AS)) \cdot exp[-V_{gS} \cdot (\frac{1}{vT} - \frac{1}{vTr}], \tag{5.43}$$

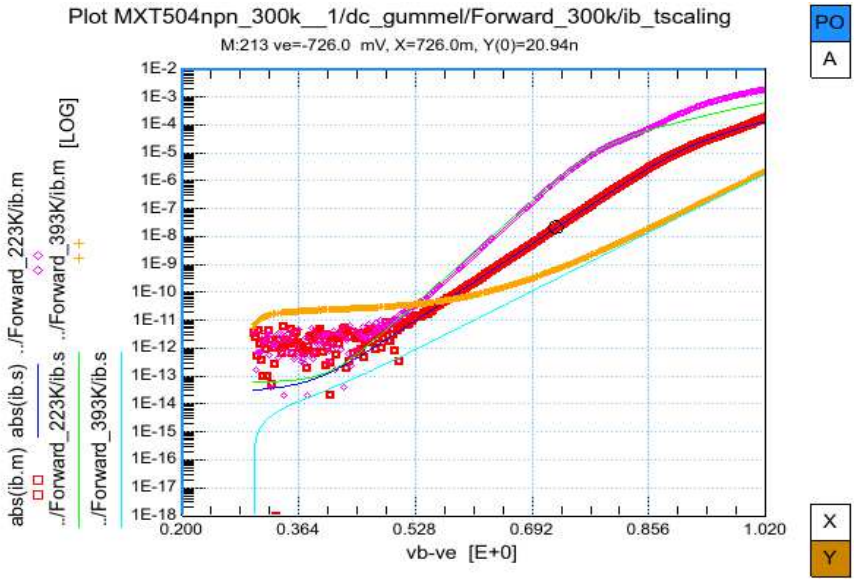

Figure 5.8: Measured(markers) and simulated(line) base current temperature scaling

we can see that I_{SsT} is decided by A_S and V_{gS}. So by optimizing these two parameters we can get a good fitting result. The result is shown in Figure 5.9.

5.2.6 DVGBR and VGC

So after fitting substrate currents in wide temperature, we need to check reverse current gain at different temperature. As is known, to make sure reverse current gain fits in wide temperature range we need to correct B_{rtI} and I_{BRT}.

$$B_{riT} = B_{ri} \cdot exp[-DVGBR * (\frac{1}{vT} - \frac{1}{vTr}], \tag{5.44}$$

$$I_{BRT} = I_{BR} \cdot tN^2 \cdot exp(-V_{gC} \cdot \frac{V_{dtINV}}{2}), \tag{5.45}$$

From these equations we can find out the B_{rtI} and I_{BRT} are decided by temperature scaling parameters $DVGBR$ and V_{gC}. When I did the B_{ri} and I_{BR} extraction, I fitted plots of I_B-I_{sub}. So here I still choose the same fitting. Plot out three I_B-I_{sub} curves at different

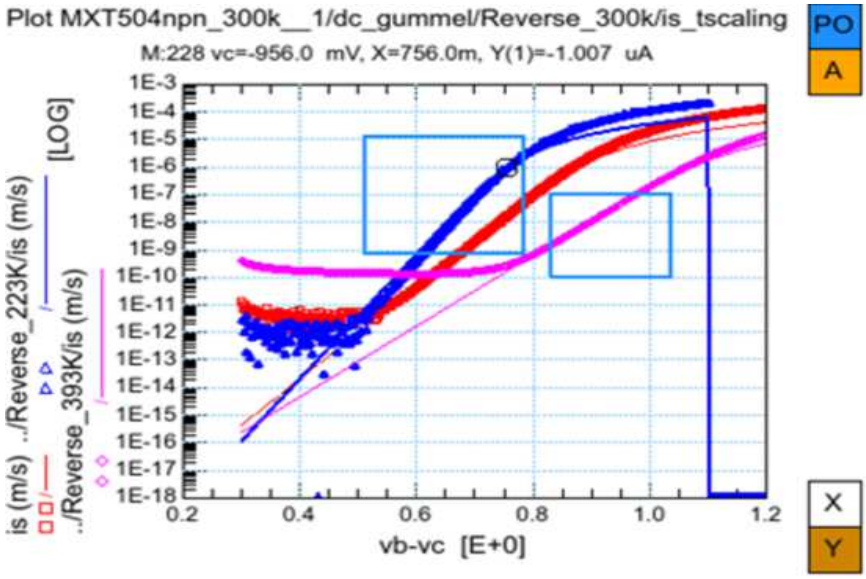

Figure 5.9: Measured(markers) and simulated(line) substrate current temperature scaling

temperatures and by optimizing these two parameters we can get a good fitting result. The result is shown in Figure 5.10.

5.2.7 AC, ATH, and AE

From Figure 5.11 to Figure 5.12 we can see the temperature scaling of dc output curves at low I_B. The result shows good fitting then we can confirm that the former temperature scaling parameters extraction is good. Now we can focus on temperature scaling of output curves at high I_B. Because output curve characteristics are mainly decided by self-heating effect and also resistances like R_{Cc} and R_{Cv}.

$$R_{CVT} = R_{CV} \cdot exp(lntN \cdot A_{epi}), \tag{5.46}$$

$$R_{CCxxT} = R_{CC} \cdot exp(lntN \cdot A_C), \tag{5.47}$$

$$R_{CCexT} = R_{CBLX} \cdot exp(lntN \cdot ACBL), \tag{5.48}$$

$$R_{CCinT} = R_{CBLI} \cdot exp(lntN \cdot ACBL), \tag{5.49}$$

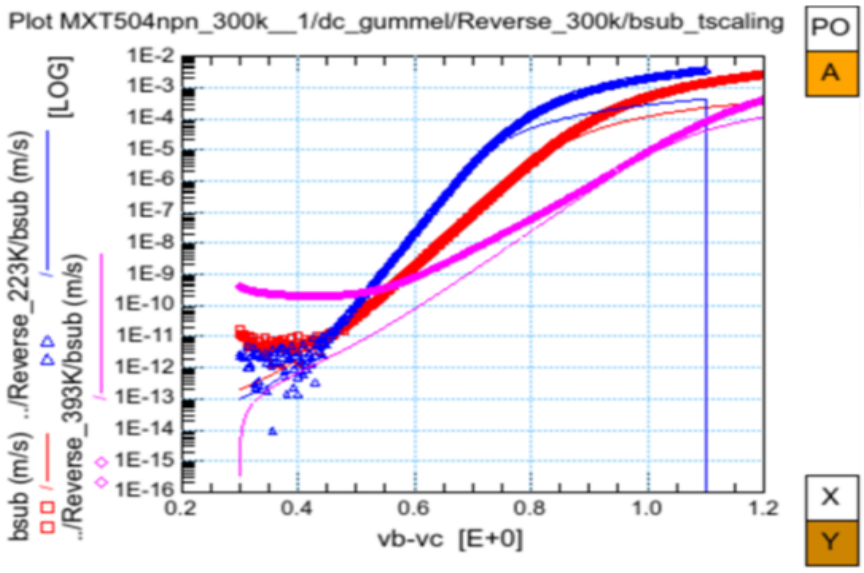

Figure 5.10: Measured(markers) and simulated(line) I_B-I_{sub} temperature scaling

At Mextram R_{CBLX} and R_{CBLI} are modeled for collector resistance besides R_{Cc}. Since we didn't consider R_{CBLX} and R_{CBLI} in this thesis so $ACBL$ is also not used in optimization and extraction for temperature scaling. Since R_{th} plays an important role in output curves, so A_{th} will be essential for output curve temperature scaling, especially at high temperature. A_E effects the temperature scaling of R_E but we need to notice that A_E is zero here. By optimizing A_E, A_C, and A_{th} we can fit dc output curves at wide range temperature. The plots are shown from Figure5.13 to Figure 5.14.

5.2.8 AEPI and DVGTE

$$\tau_{ET} = \tau_E \cdot exp(lntN \cdot (AB - 2)) \cdot exp(-DVGTE \cdot V_{dtINV}); \tag{5.50}$$

$$\tau_{epiT} = \tau_{epi} \cdot exp(lntN \cdot (AEPI - 1)); \tag{5.51}$$

Based on cutoff frequency at 300K we know it is decided by τ_B, τ_E, and τ_{epi}. From former extraction, we know the values of A_B. So now we just need to optimize A_{epi} and $DCGTE$

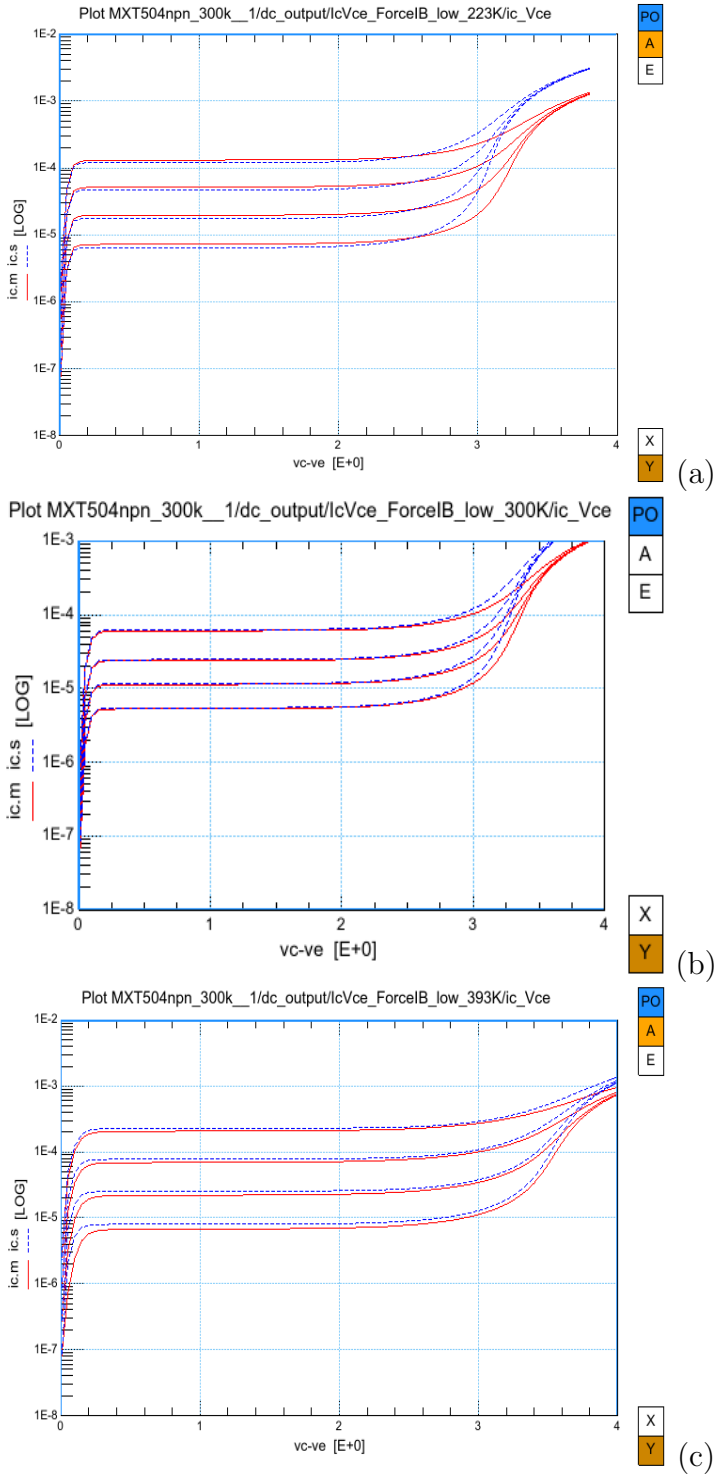

Figure 5.11: Measured (symbol) and simulated (solid line) forced I_B low I_C-V_{CE} from 223-393 K. (a) 223K. (b) 300K. (c) 393K.

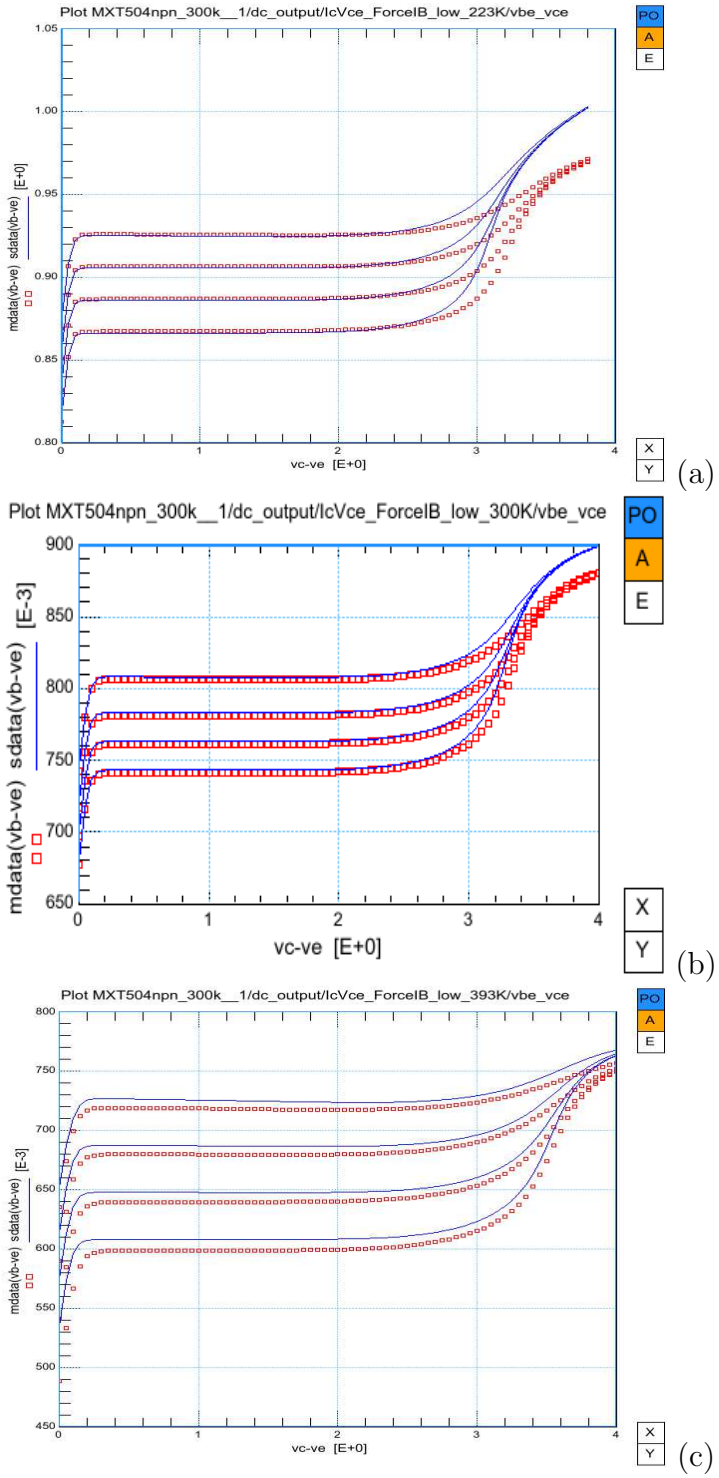

Figure 5.12: Measured (symbol) and simulated (solid line) forced I_B low V_{BE}-V_{CE} from 223-393 K. (a) 223K. (b) 300K. (c) 393K.

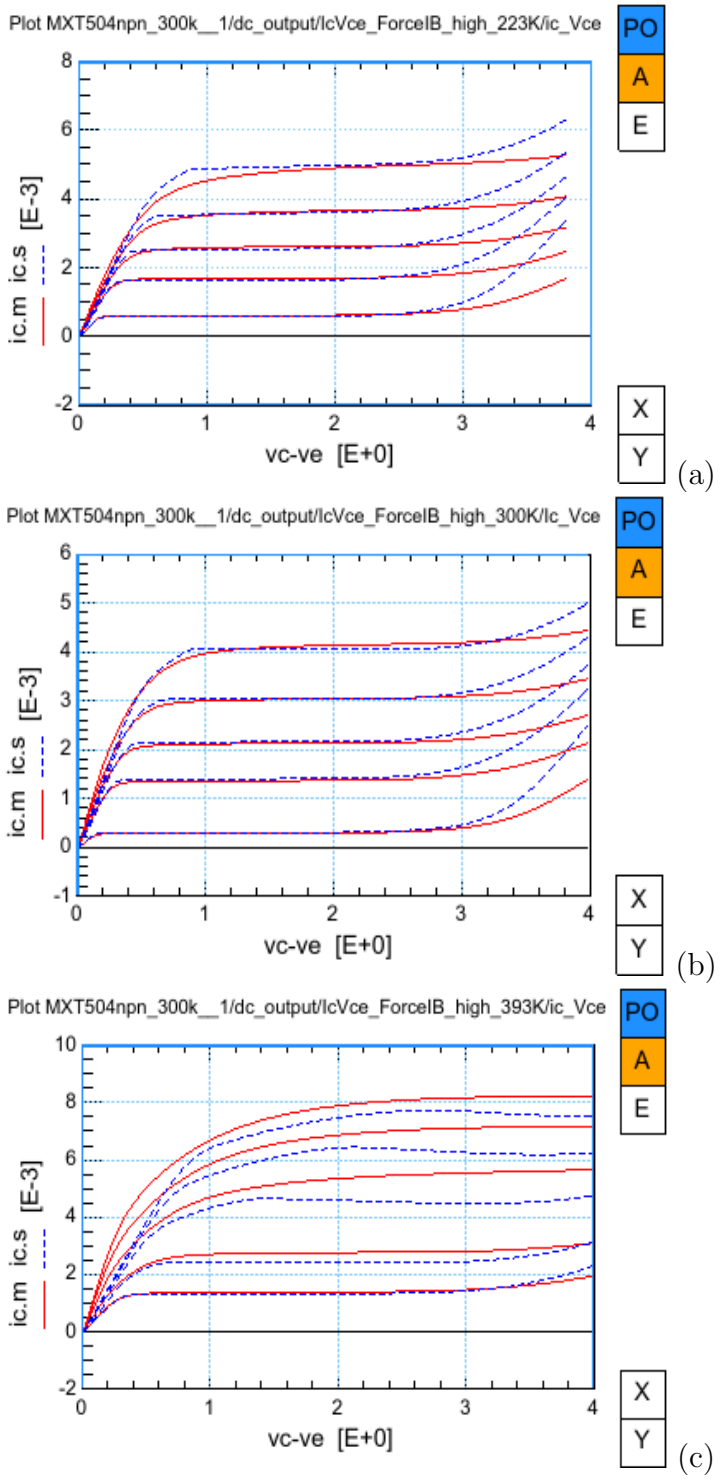

Figure 5.13: Measured (symbol) and simulated (solid line) forced I_B high I_C-V_{CE} from 223-393 K. (a) 223K. (b) 300K. (c) 393K.

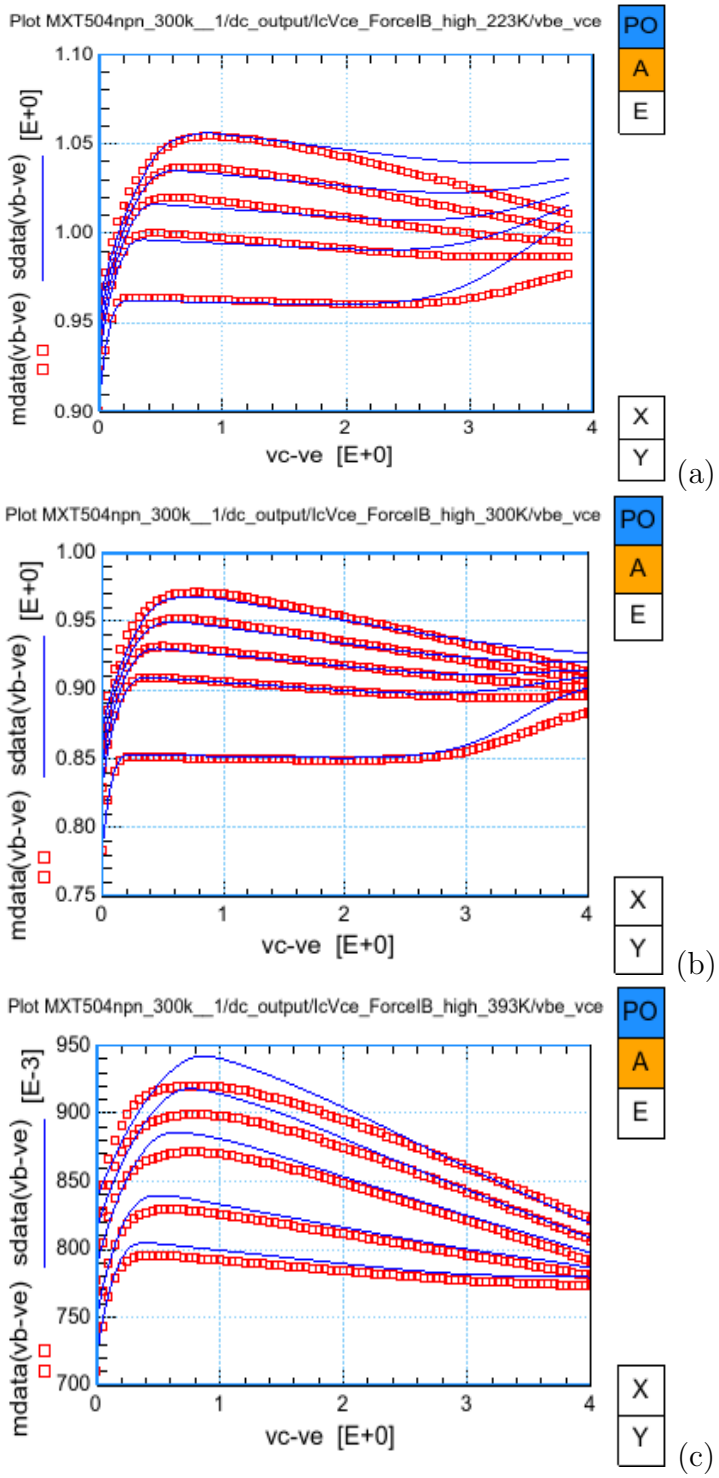

Figure 5.14: Measured (symbol) and simulated (solid line) forced I_B high V_{BE}-V_{CE} from 223-393 K. (a) 223K. (b) 300K. (c) 393K.

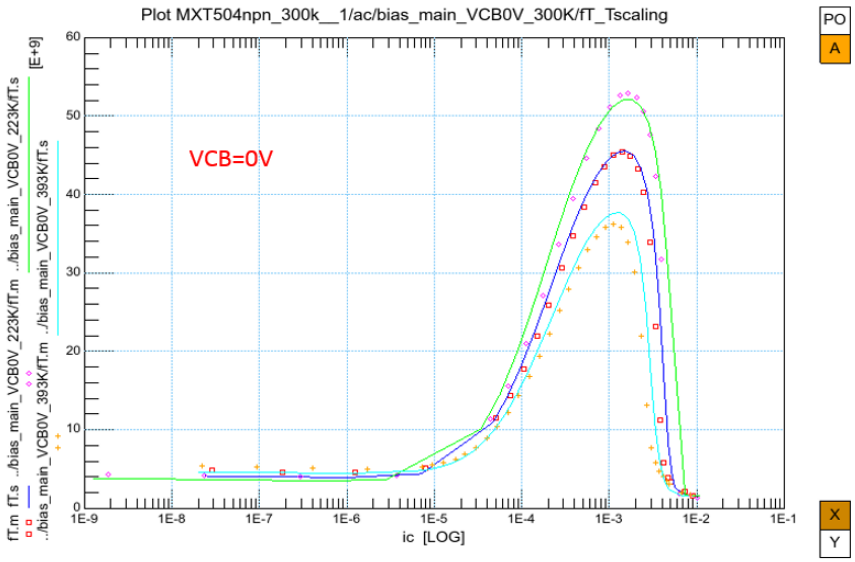

Figure 5.15: Cutoff frequency temperature scaling at V_{CB}=0V .

to fit cutoff frequency at multiple temperatures. The result is shown from Figure 5.15 to Figure 5.17 .

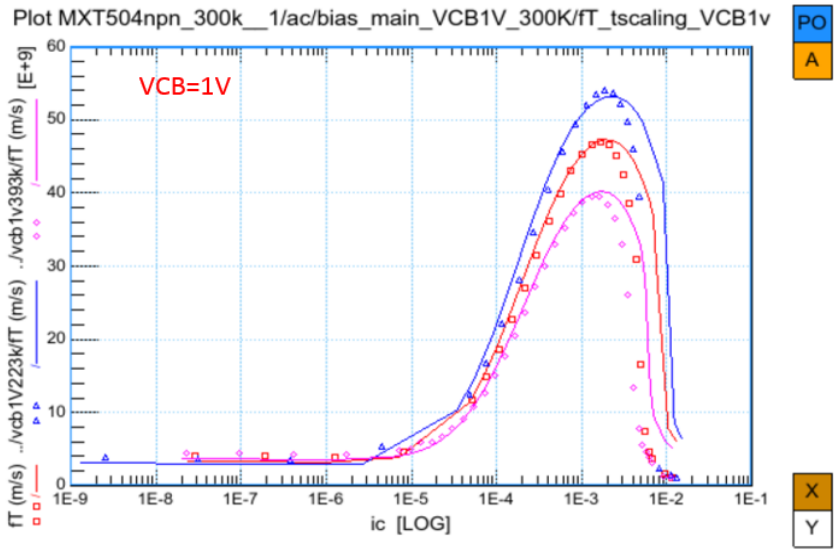

Figure 5.16: Cutoff frequency temperature scaling at V_{CB}=1V(Blue is at 223K; Red is at 300K; Pink is at 393K.)

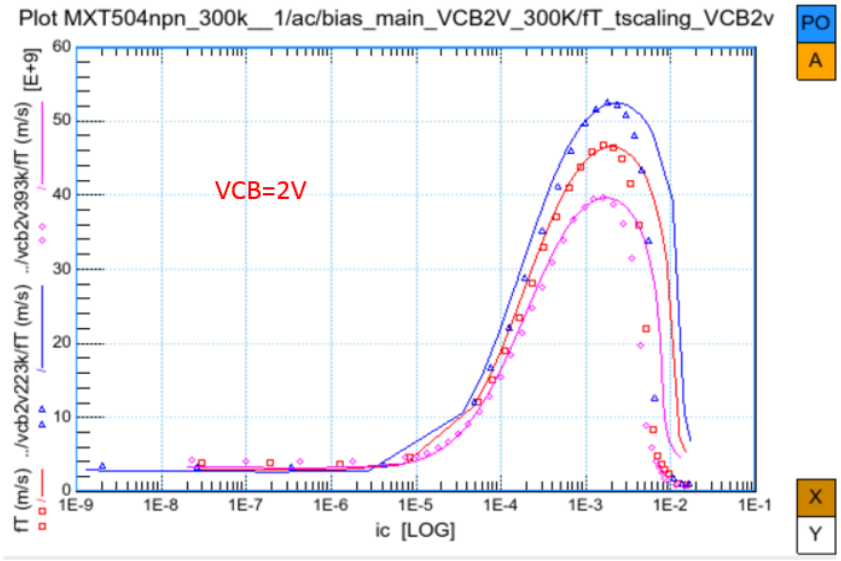

Figure 5.17: Cutoff frequency temperature scaling at V_{CB}=2V(Blue is at 223K; Red is at 300K; Pink is at 393K.)

Bibliography

[1] J.D. Cressler, "SiGe HBT Technology: A New Contender for Si-based RF and Microwave Circuit Applications," *IEEE Transactions on Microwave Theory and Techniques*, vol.46, pp.572-589, May 1998.

[2] Z. Xu, "Physics, Modeling and Design Implications of RF Correlation Noise in SiGe HBTs," *Auburn University*, 2013.

[3] J. D. Cressler and G. F. Niu, "Silicon-Germanium Heterojunction Junction Bipolar Transistors" Artech House, 2003.

[4] G. Niu, R. V. D. Toorn, J. C. J. Paasschens, W.J. Kloosterman, , *The Mextram Bipolar Transistor Model Definition*, Auburn University, 2015.

[5] Pengyu Li, "Python based Mextram Model Parameter Extraction" *Auburn University*, 2015

[6] J. C. J. Paasschens and W. J. Kloosterman, "The Mextram bipolar transistor model,level 504," Philips Nat.Lab., 2000.

[7] J. C. J. Paasschens, W.J. Kloosterman, R. V. D. Toorn, *Model Derivation of Mextram 504: The Physics behind the Model*, Koninklijke Philips Electronics, 2004.

[8] J. C. J. Paasschens,W. J. Kloosterman, and R. J. Havens, *Parameter extraction for the bipolar transistor model Mextram*, Koninklijke Philips Electronics, 2001.

[9] L. Luo, "Physics, Compact Modeling and TCAD of SiGe HBT for Wide Temperature Range Operation," *Auburn University*, 2011.

[10] G. M. Kull, L.W. Nagel, S. Lee, P. Lloyd, E. J. Prendergast, and H. Dirks,"A unified circuit model for bipolar transistors including quasi-saturation effects," *IEEE Transactions on Electron Devices*, vol. ED-32, no. 6, pp. 11031113, 1985.

[11] D. B. M. Klaassen, "A unified mobility model for device simulationII. temperature dependence of carrier mobility and lifetime," *Solid-State Elec.,*, vol. 35, no. 7, pp. 961967, 1992.

[12] I. E. Getreu,, "Modeling the bipolar transistor" Elsevier Sc. Publ. Comp., Amsterdam, 1978.

[13] Advanced Design System 1.5, "users guide.," Agilent Technologies, 2001.